

Dynamics of Rod like Particles in Supercooled Liquids - Probing Dynamic Heterogeneity and Amorphous Order

Anoop Mutneja* and Smarajit Karmakar†

*Tata Institute of Fundamental Research, 36/P, Gopanpally Village,
Serilingampally Mandal, Ranga Reddy District, Hyderabad, 500107, Telangana, India*

Probing dynamic and static correlation in glass-forming supercooled liquids has been a challenge for decades in spite of extensive research. Dynamic correlation which manifests itself as Dynamic Heterogeneity is ubiquitous in a vast variety of systems starting from molecular glass-forming liquids, dense colloidal systems to collections of cells. On the other hand mere concept of static correlation in these dense disordered systems remain somewhat elusive and its existence is still actively debated. We propose a novel method to extract both dynamic and static correlations using rod like particles as probe. This method can be implemented in molecular glass-forming liquids in experiments as well as in other soft matter systems including biologically relevant systems. We also rationalize the observed log-normal like distribution of rotational decorrelation time of elongated probe molecules in reported experimental studies along with a proposal of a novel methodology to extract dynamic and static correlation lengths in experiments.

* anoopm@tifrh.res.in

† smarajit@tifrh.res.in

INTRODUCTION

Being structurally disordered, constituent particles or molecules in both the liquid and glass phases, experience variable local environments. This can be easily ignored for high temperature liquids but for supercooled liquids it manifests itself in spatial distribution of particle's mobility, from nearly stuck to fairly moving. This in turn gives rise to complex behaviour in their bulk properties like viscosity, structural relaxation time as well as diffusion constant. All of these complex dynamical behaviour is termed in literature as Dynamical Heterogeneity (DH)[1, 2]. It has been shown that the slow and fast moving local regions form clusters [3–5] which lead to strong spatial variation in local relaxation times of the system. These spatial variation in local relaxation times adds up to an overall non-exponential relaxation, observed in various experimental [6] and simulation [7] studies. Non-Gaussian behaviour with universal exponential tail [8] in the distribution of particles' displacements or the van Hove function (See SI for definition) is also a direct manifestation of the same dynamical heterogeneity.

On the other hand, in the supercooled regime, the relaxation time or the viscosity of the system also increases very drastically with little decrease (increase) in temperature (density). In [9–11], it was argued that the growing dynamical heterogeneity length scale is not causally related to the growth of the timescale or viscosity. Thus existence of yet another length scale became necessary to rationalize the rapid growth of relaxation time and in [9] it was proposed that a static length scale also grows with decreasing temperature. It is important to note that existence of such a static length scale is consistent with the predictions of Random First Order Transition (RFOT) Theory [12, 13]. In [14], a new correlation function, known as Point-to-Set (PTS) correlation function (see SI for definition), was proposed and estimated in various model glass-forming liquids to extract the static length scale. Growth of the PTS length scale is found to be connected with growth of the relaxation time with supercooling. Various other measures of similar static length scale are also found to be consistent with each other [15, 16]. The underlying structural order related to PTS length scale is often referred to as "Amorphous Order". It is now well established that there are indeed two different length scales that grow while approaching glass transition [17, 18], although a possible mutual relation between these two length scales remain poorly understood[19]. It is important highlight that there are lot of effort of identify structural motifs that can be related to the growth of static length scale [20, 21]

To quantify dynamic heterogeneity, one often measures the length scales and time scales of different mobility clusters and their variation while approaching glass transition. The dynamical heterogeneity length scale, ξ_D is computed in general using [22, 23] the peak value of fluctuations of the total mobility characterized by four-point susceptibility, $\chi_4(t)$ (see SI for definition) which is often assumed to be related to ξ_D as $\chi_4^P \sim \xi_D^{2-\eta}$ with η being an unknown exponent. ξ_D can also be computed from the spatial correlation in the particles' mobility field[24–26]. Recently, in Ref. [27, 28], the non-Gaussian nature of the van Hove function is used to probe the dynamical heterogeneity length scale very efficiently by systematically coarse-graining the system at varying length scales. The idea is that upon coarse-graining over the length scale comparable or larger than dynamical heterogeneity length scale, one would expect that the distribution of particle's displacement or the van Hove function will tend to become Gaussian. In this work we have studied dynamics of rod-like particles in supercooled liquids with varying length of the rods to similarly probe response of the system at varying coarse-graining length scales and extract the dynamical heterogeneity length scale. Thus, this method might become more accessible to experiments for measuring the dynamic heterogeneity length scale in various molecular glass-forming liquids as well as in colloidal glasses.

Direct experimental measure of χ_4 or displacement-displacement correlation function for molecular liquids is not possible as one needs to spatially and temporally resolve the trajectories of all constituents particles in a system. Although similar measurement can be done for colloidal or granular systems [29–33]. Thus for molecular liquids, one often measures $\chi_4(t)$ indirectly as shown in Ref. [34]. It was shown that a suitable dynamical response function $\chi_x(t)$ to an induced perturbation variable, ' x ', e.g. density fluctuations in colloidal glasses or temperature fluctuation in molecular glass-forming liquids will be related to $\chi_4(t)$. One thus estimates $\chi_4(t)$ by using linear response formalism and fluctuation theory, but an accurate estimate of the length scale will still not be possible as the exponent, η is apriori unknown [35–37]. Similarly, experimental measure of growing amorphous order is also very limited and a direct evidence of such a growing static length scale came from the measurement of fifth-order dielectric susceptibility ($\chi_5(t)$) in supercooled glycerol and propylene [38] and via random pinning using holographic optical tweezers [39]. The intricacy of the experimental measurement immediately tells us that an accurate measurement of growing amorphous order is still very hard. Thus it is not very surprising that we do not have strong experimental evidence of growth of both dynamical heterogeneity length scale as well as the static length scale of amorphous order in molecular glass-forming liquids. An experimentally realizable proposal for possible measurements of these two important length scales will definitely be of importance for understanding the puzzle of glass transition.

In particular, the experiments on the rotational dynamics of a single probe in the form of dye molecules[40] and nano-rods [41] are very encouraging. In [41], the rotational correlation time (τ) of gold nano-rods in supercooled glycerol are measured. This time scale is found to increase with decreasing temperature. The distribution of τ is surprisingly found to be log-normal in nature whose variance increases with decreasing temperature, indicating a possible increase in dynamic heterogeneity. Similar results were also obtained for single dye molecule experiments in supercooled glycerol [40]. Note that nano-rods are of much larger in size than usual dye molecules. The appearance of log-normal distribution in rotation time itself conveys the finite probability of rod or molecule to be rotationally immobile or just vibrating for most of the time. This also implies the existence of heterogeneity at both the length scales of gold nano-rod and of single dye molecule. Although existence of dynamical heterogeneity is evident

from these experimental measurements, a direct measure of dynamical heterogeneity length scale is still not available. In this work, we propose that growth of both dynamical and static length scales can be obtained using similar single molecule probe experiments by systematically varying the length of probe molecules and studying their rotational relaxation dynamics.

Our proposed methodology is simply to study the rotational dynamics of rod-like probe molecules as done experimentally in [40, 41] but look at the changes in dynamics as one varies the length of probe rod as schematically shown in the top left panel of Fig:1. To quantify the heterogeneity in dynamics, we use non-normal parameter for rotational diffusion of the rods. This is similar to the Binder cumulant or the non-Gaussian parameter usually studied in the context of studying dynamic heterogeneity in systems with spherical particles. In Ref. [42], it has been analytically shown that the following will be the appropriate non-normal parameters for distributions $P_{2D}(\phi, t)$ and $P_{3D}(\theta, t)$, where $\phi(t) \in [-\pi, \pi]$ is the polar angle in 2D system and $\theta(t) \in [0, \pi]$ is the azimuthal angle in 3D system (assuming the rods are initially placed along the positive x-axis in 2D ($\phi = 0$) and along positive z-axis ($\theta = 0$) in 3D).

$$\alpha_{rot,2D} = \frac{1}{3} \frac{\langle |\hat{u}(t) - \hat{u}_0|^4 \rangle}{(\langle |\hat{u}(t) - \hat{u}_0|^2 \rangle)^2} - \frac{1}{24} \langle |\hat{u}(t) - \hat{u}_0|^2 \rangle \times (\langle |\hat{u}(t) - \hat{u}_0|^2 \rangle - 8) - 1 \quad (1)$$

$$\alpha_{rot,3D} = \frac{1}{2} \frac{\langle |\hat{u}(t) - \hat{u}_0|^4 \rangle}{(\langle |\hat{u}(t) - \hat{u}_0|^2 \rangle)^2} + \frac{1}{6} \langle |\hat{u}(t) - \hat{u}_0|^2 \rangle - 1. \quad (2)$$

$\hat{u}(t)$ is the orientation unit vector of rod at time ‘t’ and \hat{u}_0 is the orientation vector at time $t = 0$, implying $\theta = \cos^{-1}(\hat{u}(t) \cdot \hat{u}_0)$ in 3D and $\phi = \cos^{-1}(\hat{u}(t) \cdot \hat{u}_0)$ in 2D. These non-normal parameters of the distributions $P_{2D}(\phi, t)$ and $P_{3D}(\theta, t)$ will go to zero if there is no heterogeneity present in the system. Thus value of this non-normal parameter would then quantify the variation in rotational diffusion constant of the rod and hence the dynamic heterogeneity.

If the liquid is at high temperature (or low density) then one expects the non-normal parameters, $\alpha_{rot,2D}(t, T)$ or $\alpha_{rot,3D}(t, T)$ to remain zero for all rod lengths and at all times, but for supercooled liquid in the presence of dynamic heterogeneity, the non-normal parameters will be non-zero and one can expect to see a maximum at time scale around $t = \tau_\alpha$ similar to $\chi_4(t, T)$. One also expects that peak value of the non-normal parameters ($\alpha_{rot,2D}^P$, $\alpha_{rot,3D}^P$) should grow with decreasing temperature consistent with the growth of heterogeneity in the system. It is somewhat intuitive to understand that the values of $\alpha_{rot,2D}^P$, $\alpha_{rot,3D}^P$ too will decrease with increasing rod length as the rod will now experience the collective dynamical response of the surrounding liquid medium averaged over a volume of linear size comparable to the length of rod. Thus in principle, we will have the measure of the heterogeneity at various length scales using which the calculation of dynamic heterogeneity length scale should not be very difficult. Also, as Finite-Size-Scaling (FSS) of structural relaxation time τ_α [9] gives us static length scale we can be hopeful to be able to obtain the same from the rotational correlation time of the rod and its distributions along with a possible understanding of the experimentally observed log-normal distribution of rotational correlation time [40, 41] of the probe molecules.

In this work, we have done extensive simulation of three model glass-forming liquids as discussed in detailed in the Method section. These three models are referred in the rest of the article as **3dKA**, **3dHP** and **2dmKA** models. The details of the parameters of the models and the techniques used in performing Molecular Dynamics simulations in the presence of the rod-like particles can be found in the Method section. The rest of the paper can be broadly separated into two parts. In the first part, we discuss in detail the scaling analysis performed to extract the dynamical heterogeneity length scales from the rod length dependence of rotational non-normal parameter both in two and three dimensional systems. Then in the second part, we discuss First Passage time (FPT) distribution of the rod molecules in the liquid with increasing supercooling and how one can extract the static length scale from that.

RESULTS

Non-Normal Parameters and Dynamic Heterogeneity Length

Fig. 1(b) shows the time evolution of non-normal parameter $\alpha_{rot,3D}$ for 3dKA model at $T = 0.50$. Clearly it shows a maximum at $t \sim \tau_\alpha$ indicating that such analysis indeed picks up the heterogeneity of the parent liquid. It can also be seen that the value of peak goes down with increasing rod length which validates the correctness of our assumption that the dynamically heterogeneous environment experienced by the rod particles gets averaged out with increasing length of the rod. In the inset of Fig: 1(c) we show similar data for a given rod with decreasing temperature. This results show the increase of heterogeneity in parent liquid at the probing length scale of the order of the rod length with decreasing temperature. Fig: 1(c) shows the variation of $\alpha_{rot,3D}^P$ as a function of rod length, for different temperatures for 3dKA model. Results are very similar for other models as shown in SI.

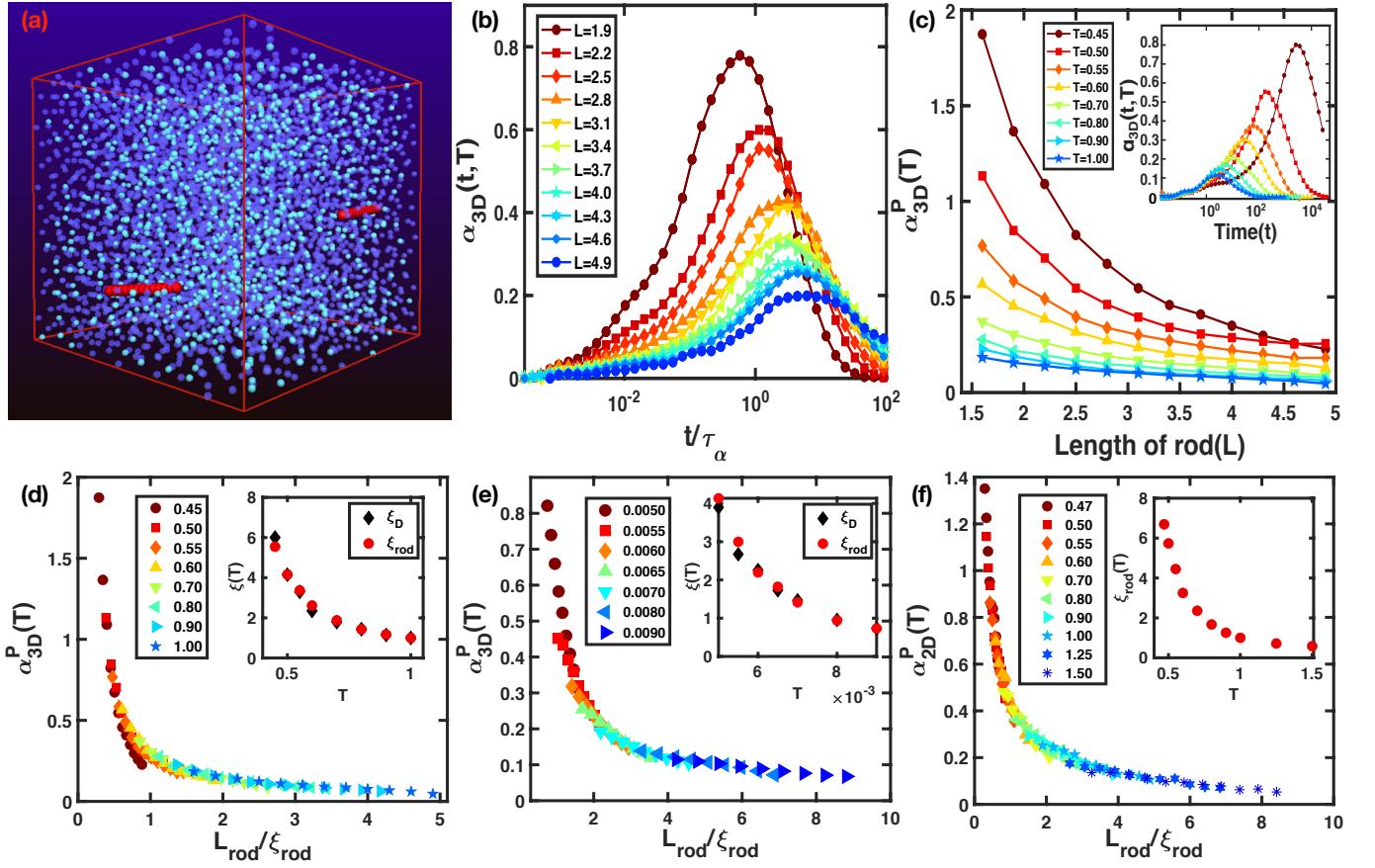


FIG. 1. (a) Schematic representation of rod particles in the supercooled liquid medium. (b) Evolution of Non-Normal parameter ($\alpha_{rot,3D}(t)$) for different size of the rod in 3dKA supercooled liquid model at temperature $T = 0.50$. Inset of (c) Evolution of Non-Normal parameter ($\alpha_{rot,3D}(t)$) for rods of length $L_{rod} = 2.5$ in the same supercooled liquid model at different temperatures. (c) Variation in peak value of Non-Normal parameter $\alpha_{3D}^P(T)$ with length of the rod in 3dKA system at different supercooling temperatures. Bottom panels: Collapse of non-normal parameter obtained by scaling the rod length with appropriate correlation length scale ξ_{rod} for all three systems (3dKA, 3dHP and 2dMKA from (d) to (f)). In the insets of these plots, the scaling length scale is compared with the dynamic length scale of the parent liquid obtained by other conventional methods [28] (see text for details). Both the length scales are found to be in good agreement with each other.

The dynamic heterogeneity as probed by the rod decreases with increasing rod length, one can expect that the behaviour changes when the rod length is comparable to the dynamic heterogeneity length scale, ξ_D at the studied temperature. Thus one can attempt to do a scaling plot of the non-normal parameters for different lengths of the rod and temperatures using the dynamical heterogeneity length scale. If the physics is governed by the dynamical heterogeneity length scale then one would expect a master plot when $\alpha_{rot,3D}^P$ or $\alpha_{rot,2D}^P$ is plotted as a function of $L_{rod}/\xi_D(T)$, where L_{rod} is the length of the rod. Fig. 1 (bottom panel) show the master curves for 3dKA, 3dHP and 2dMKA model (left to right). Length scale, $\xi_{rod}(T)$ is obtained by demanding the best data collapse. In the insets of Fig. 1 (bottom panel), ξ_{rod} is plotted along with the dynamic length scale, ξ_D obtained by other conventional methods [10, 11]. The collapse obtained for all of the models are observed to be good along with the fact that the length scale obtained using this scaling analysis matches very well with the dynamic heterogeneity length scale obtained using other methods. The ξ_D data reported in this article is taken from Ref.[28]. This gives us the confidence that rod-like probe molecules can indeed be a good probe of the dynamical heterogeneity in glass forming liquids. Thus it is needless to mention that the proposed method can be easily realized in experiments in the light of the already existing experimental results [40, 41]. Only a systematic variation of the probe molecules is required to obtain the coveted length scale in molecular glass-formers.

First Passage Time Distribution and Static Length Scale

We now focus our attention on the decorrelation time of these rod-like particles immersed in a supercooled liquids with different amount of supercooling as done experimentally in Refs. [40, 41]. In these experimental studies, it was found that the

distribution of decorrelation time is log-normal in nature and the width of the distribution increases with decreasing temperature. To understand this experimental observation, we looked at the decorrelation time of our rod-like particles in the supercooled liquid medium at different temperatures and one indeed finds that the distribution is close to log-normal at least within the error bar of the simulation data. To gain further insight, we look at the statistics of “First Passage Time (FPT)” distribution of these rod-like particles. First Passage distribution $F(t, \phi_c)$ in 2D is defined as the probability of rod crossing the angle $\phi = \phi_c$ at a time t for the first time. If we unfold the ϕ -coordinate such that $\phi \in (-\infty, +\infty)$, then this distribution is same as that of well known FPT distribution of the one dimensional Brownian particle i.e $F(t, x_c) = \frac{x_c}{\sqrt{4\pi Dt^3}} e^{-x_c^2/4Dt}$. But the quantity of interest here would be the distribution of decorrelation time i.e $F(t, \pm\phi_c)$. This $F(t, \pm\phi_c)$ is exactly the distribution of time taken for a one dimensional Brownian particle to leave the bounded region $[-\phi_c, +\phi_c]$ while starting from $\phi = 0$. In SI, we have shown the FPT distribution of such a Brownian rod. Next we compute such distribution of FPT of rod in liquid medium in both two dimensions(2D) and three dimensions (3D).

For Brownian motion of rod in 2D, one can easily verify that

$$\mathcal{P}_c(\phi, t) = \frac{1}{\phi_c} \sum_{n=0}^{\infty} \cos\left(\frac{(2n+1)\pi\phi}{2\phi_c}\right) e^{-\frac{(2n+1)^2\pi^2}{4\phi_c^2}Dt} \quad (3)$$

satisfies the diffusion equation (see Eq:SI-7) with two absorbing boundaries at $\phi = \pm\phi_c$. In this solution each eigenstate decays exponentially in time with decay rate $\frac{(2n+1)^2\pi^2}{4\phi_c^2}$, thus only $n = 0$ eigenstate would contribute to the survival probability (probability that particle is not yet absorbed) at large times, implying,

$$S(t) \propto e^{-\frac{D\pi^2}{4\phi_c^2}t} = e^{-t/\tau}. \quad (4)$$

Thus the first passage time which can be obtained from survival probability via differentiation will also be exponential at long time. The exponential fit to the large time part of the distribution of FPT of the Brownian rod is found to be very good as shown in SI. Also one can obtain following solution for $\mathcal{P}_c(\phi, t)$ by the method of images,

$$\mathcal{P}_c(\phi, t) = \frac{1}{\sqrt{4\pi Dt}} \sum_{n=-\infty}^{\infty} (-1)^n e^{-\frac{(\phi+2n\phi_c)^2}{4Dt}} \quad (5)$$

Note that the two solutions, Eq.3 and Eq.5 are same but represented via two different series. Readers are encouraged to read

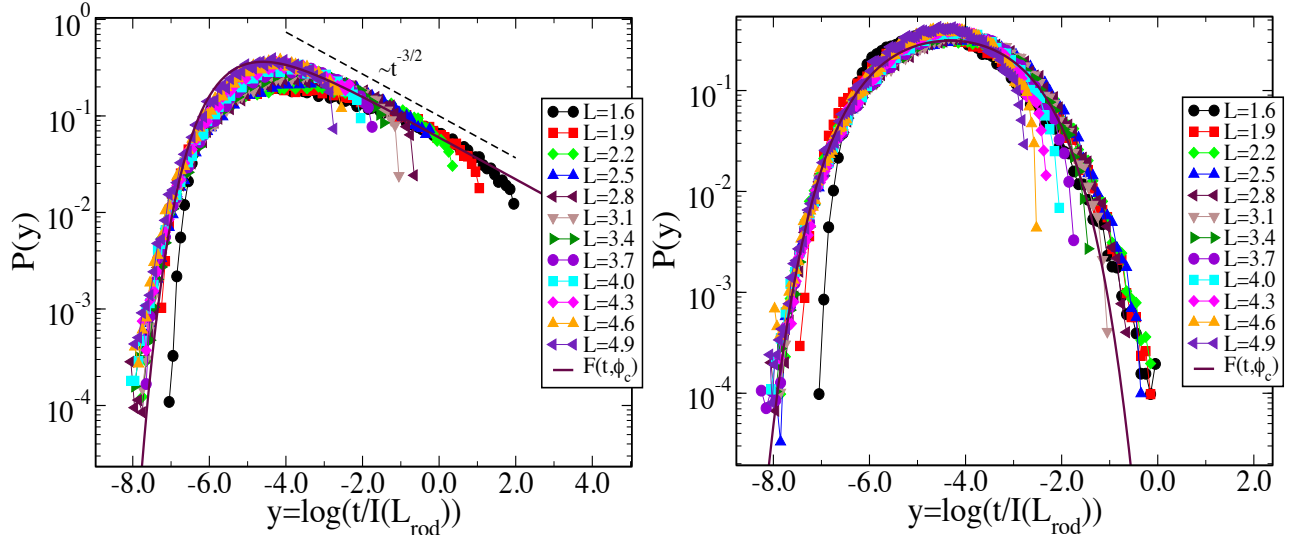


FIG. 2. Left panel: Distribution of first passage times for rods of various lengths scaled by moment of Inertia ($I(L_{rod})$) in 2dMKA system at temperature $T = 1.5$ (high temperature) with one absorbing boundary at $\phi = \phi_c$. Note, for this calculation we have use unbounded coordinates, i.e $\phi \in [-\infty, +\infty]$. Right panel: Distribution of first passage times for rods of various lengths scaled by moment of Inertia, $I(L_{rod})$ in 2dMKA system at temperature $T = 1.5$ (high temperature) with two absorbing boundaries at $\phi = \pm\phi_c$. The bold line is the fitting to Eq.8.

Ref.[43] for details. In the limit of small time, only $n = 0$ term would contribute which would lead us to following expression

of survival probability at small times.

$$S(t \rightarrow 0) \propto \frac{\sqrt{4\pi Dt}}{\sqrt{4\pi Dt}} \operatorname{erf}\left(\phi_c \sqrt{4Dt}\right). \quad (6)$$

On differentiating this survival probability with a negative sign would give us first passage time distribution to be,

$$F(t \rightarrow 0, \pm\phi_c) \propto \frac{\phi_c}{\sqrt{4\pi Dt^3}} e^{-x_c^2/4Dt} \quad (7)$$

Thus the approximate closed form for the distribution, $F(t, \pm\phi_c)$ of rod and the exact series solution followed from Eq:3 are given by the following expressions

$$F(t, \pm\phi_c) \propto t^{-\beta} e^{-\alpha/t} e^{-t/\tau} \quad (8)$$

$$F(t, \pm\phi_c) = \frac{\pi D}{\phi_c^2} \sum_{n=0}^{\infty} (-1)^n (2n+1) e^{-\frac{(2n+1)^2 \pi^2 D t}{(4\phi_c^2)}} \quad (9)$$

With this exact solution we can obtain the mean first passage time to be $\langle t \rangle = \phi_c^2/2D$. If we introduce a new variable $y = \log(Dt)$ where t is the first passage time then, the distribution $P(y)$ would be independent of D , hence independent of rod length and temperature. This also implies that diffusion constant D would only change the mean of $P(y = \log(t))$ and not the shape of distribution for spatially homogeneous diffusion as is the case in pure Brownian motion or in high temperatures liquid state. As shown in SI rod length dependence of diffusion constant goes as $D(L_{rod}) \sim 1/I(L_{rod})$ with $I(L_{rod})$ being the moment of inertia of the rod. So, similarly $P(y)$ with $y = \log[t/I(L_{rod})]$ would be independent of rod length. So we can subtract out this obvious rod length scaling in order to understand the effect of supercooled liquid environment on the FPT distributions at various length scales.

The functional fit using Eq.8 for the FPT distribution of the Brownian rod with two absorbing boundaries and exact solution Eq: 9 is found to be very good as shown in SI and the value of exponent β comes out to be $\beta = -0.5$ for 2D and $\beta = -1.0$ for 3D (3D case is discussed later) along with exponential decay. In Fig. 2, the distributions of first passage time of rods scaled with their moment of inertia ($I(L_{rod})$) are shown. Left panel shows the distribution if one considers only one absorbing boundary at $\phi = \phi_c$ where $\phi \in [-\infty, +\infty]$ and the right panel shows $F(t, \pm\phi_c)$ for two absorbing boundaries. These results are obtained by simulating rods of various lengths in 2dmKA system at high temperature $T = 1.5$. Long time behaviour in Fig:2 left panel fits very well with $t^{-3/2}$ as expected, while the fitting of Eq.8 in right panel of Fig. 2 is also found to be very good.

Unlike in 2D case, the first passage distribution in 3D is not analytically calculable. So we have solved it numerically (see SI for details). $F(t, \theta_c)$ in 3D is defined as the probability that rod crosses the angle $\theta = \cos^{-1}(\hat{u}(t)\hat{u}(0)) = \theta_c$ at time t for the first time. So basically we need to solve for density $\mathcal{P}_c(\theta, \phi, t)$ in the 3D rotational diffusion equation for a rod with absorbing cone at $\theta = \theta_c$, from there one gets the survival probability and eventually the first passage distribution (See SI for detailed discussion). The first passage distribution decays exponentially for 3D case as well, thus Eq 8 will describe the first passage distribution of rod in 3D. Fig. 3 (a) & (b) are the unscaled and scaled first passage distributions of rods immersed in 3dKA model system at temperature $T = 2.0$ (high temperature). One sees similar results for 3dHP model as well.

Effect of Supercooling on FPT distribution: Still now we have looked at the FPT distributions for rods in 2D as well as in 3D systems at relatively high temperature where effect of supercooling can be ignored. If we now look at low temperature regime, we find distributions to develop shoulders at smaller time as shown in bottom panels of Fig.3. These are the scaled distributions of log of first passage times for rods in 3dKA system at $T = 1.0$ and $T = 0.5$ temperatures respectively. It is interesting to see that they broaden at small time regime for shorter rods and eventually converge to same asymptotic distribution for larger rods. These results can be rationalized if one assumes that the whole system is made of many domains of different mobilities as envisaged by RFOT theory as “mosaic” picture of supercooled liquid state. Since a smaller size rod can partially fit in one or two such patches it can have larger instantaneous torques and thus faster diffusion. On contrary, a larger rod would be in many such patches thus would show the bulk like homogeneous behaviour. Skewness of the distribution, $P(\log(t), \pm\phi_c)$ can then be a good measure of this local order at a length scale comparable to the size of the probe rod. Thus by measuring the skewness of the distribution of FPT for various lengths of the rod at different temperatures, one would be able to extract the length scale of amorphous order by performing systematic scaling analysis.

In top panels of Fig.4, we have shown the negative of skewness (χ_{FPT}) of the distribution shown in Fig.3 for 3dKA (top left), 3dHP (top middle) and 2dmKA (top right) models respectively. We have done the scaling collapse of the data to obtain the underlying length scale. We just scaled the x axis by a suitable choice of the length scale and plotted the data as a function of $L_{rod}/\xi_{rod}^S(T)$. The data collapse obtained is reasonably good and the corresponding length scale is plotted in the insets along with the static length scale obtained using other conventional methods like Point-to-Set (PTS) method and finite size scaling

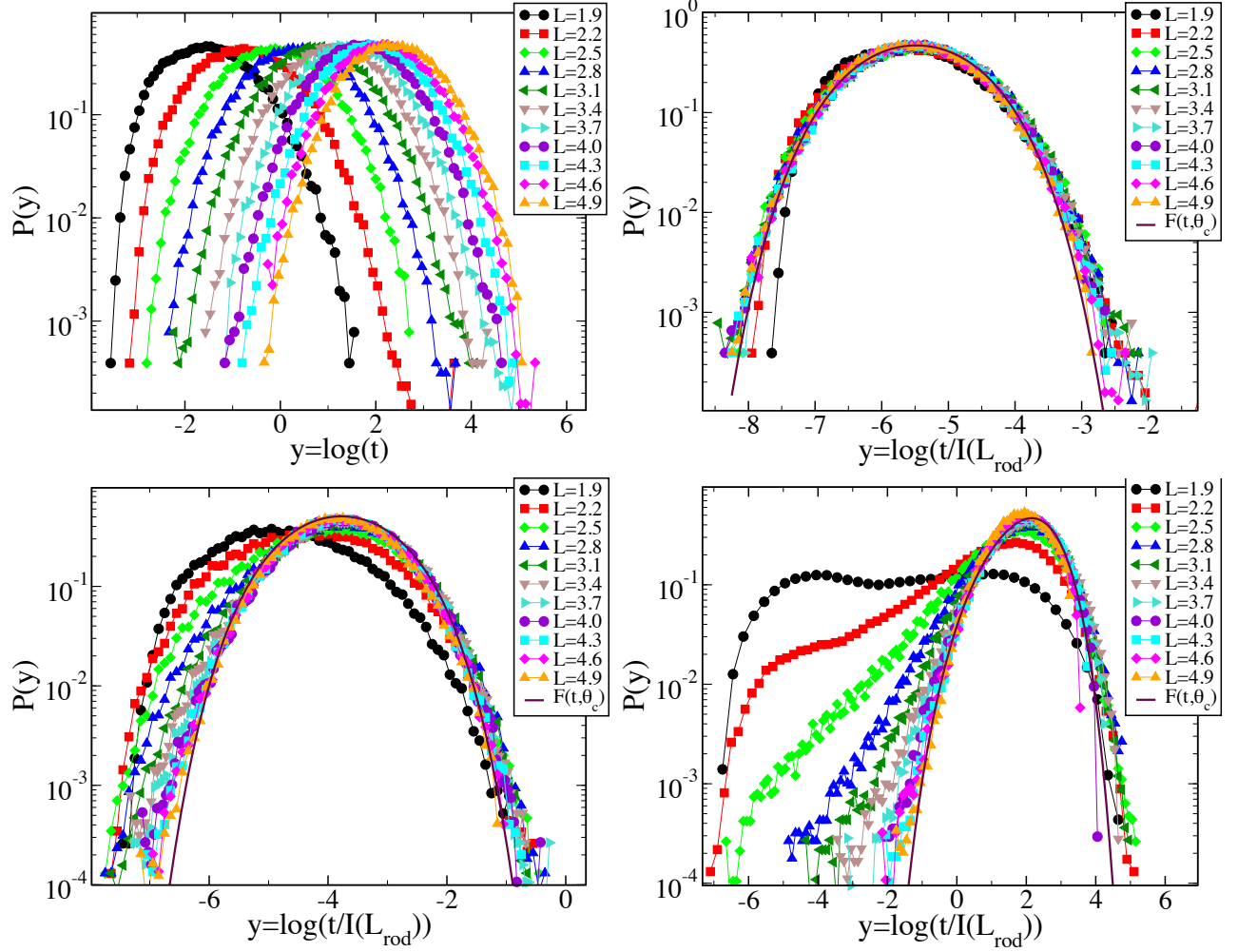


FIG. 3. Top panels: Distribution of unscaled (left) and scaled (right) first passage times (scaled with moment of inertia) for rods of various lengths in 3dKA system at temperature $T = 2.0$ (high temperature) with absorbing boundary at $\theta_c = \pi/8$. Bottom panels: Distribution of scaled first passage times (scaled with moment of inertia) for rods of various lengths in 3dKA system at temperature $T = 1.0$ (left) and $T = 0.5$ (right) (low temperatures) with absorbing boundary at $\theta_c = \pi/8$. Solid lines in these figures are fit to the Eq.8.

(FSS) of α -relaxation time of the systems[44]. Near perfect match of the temperature dependence of ξ_{rod}^s with that of PTS length scale, suggests that first passage time distribution of the rod indeed captures the static length scale in the system.

Existing Experimental Results: After understanding the underlying relationship between skewness of the distribution of first passage time or the rotational relaxation time of the rods with the static correlation length of the host supercooled liquid medium, we turn our attention to reanalyze the existing experimental results reported in Ref.[40]. In right panel of Fig.5 we show the rescaled distribution of rotation relaxation time, τ of the probe dye molecule in supercooled glycerol, scaled by the time at which the peak appears. The distribution clearly shows that with increasing supercooling $P[\log(\tau/\tau_R)]$ starts to show shoulder as seen in simulation results for small or intermediate size rod length at low temperatures as shown in the right panel of the same figure. In the inset of the left panel, we show the calculated skewness from experimental data, χ_{FPT} which seems to decrease very systematically with increasing temperature in complete agreement with our simulation results (see the inset of right panel). This also confirms the growth of amorphous order in supercooled glycerol as suggested in Ref.[38]. In the right panel figure, we show how the distribution of first passage time changes with temperature for a rod length of 2.8 in 3dKA model. The distributions are scaled by $\tau(T)$, the time at which the peak of the distribution appears at that temperature. This simple rescaling collapses the large time part of the distribution completely across different temperatures, only smaller timescale part of the distribution shows gradual growth of a shoulder with decreasing temperature. The inset shows the skewness of the distributions. The striking similarity between experimental data and simulation data are indeed very encouraging. If one does similar analysis of the experimental data of rotational correlation time of gold nanorod in supercooled glycerol from Ref.[41],

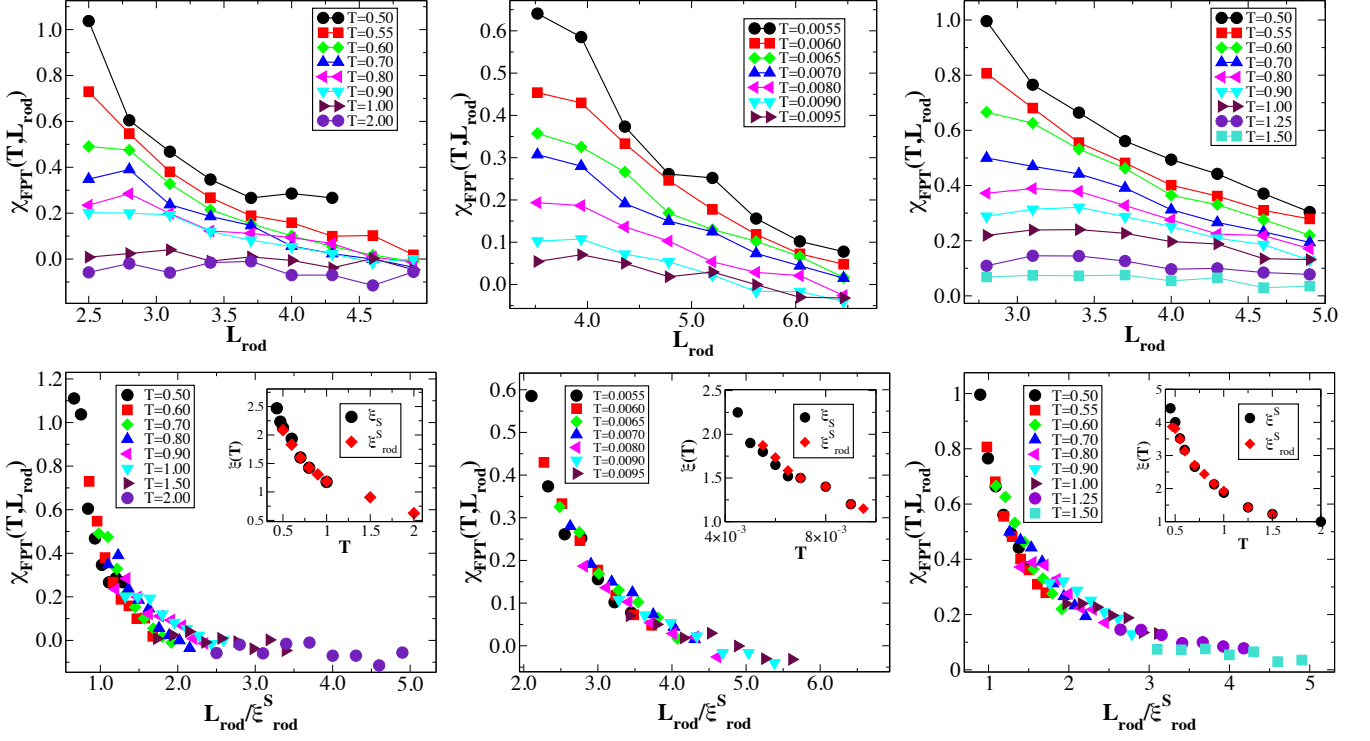


FIG. 4. Top panel: Variation in negative of skewness (χ_{FPT}) of distribution $P(\log(t))$ with rod length where t is first passage time of rod immersed in a liquid modelled by 3dKA (left), 3dHP (center) and 2dMKA (right) systems at various supercooling temperatures. Increase in skewness (building up of shoulder in small time regime) with decreasing rod length and increasing supercooling can be clearly seen, which suggests the increase in strength of structural order at length scale of rod. Bottom panel: Scaling collapse of χ_{FPT} obtained by scaling rod length with appropriate system length scale $\xi_{rod}^S(T)$ to obtain a master curve for 3dKA (left), 3dHP (center) and 2dMKA (right) model systems. The comparison of this obtained length scale is done with static length scale ξ^S obtained with traditional methods like PTS and Finite-Size-Scaling (FSS) of τ_α in the respective insets (data taken from Ref: [44]).

then one sees very little change in the skewness of the distribution (see SI). This is also in good agreement with our results as it suggests that for larger size probe molecules (gold nanorod is much larger than dye molecule) the skewness will be smaller. In bottom panel, we show the dependence of skewness, χ_{FPT} for all the model systems at different length of the rod as well as at different temperatures. χ_{FPT} plotted as a function of ξ_{rod}^S/L_{rod} seems to show a power law relation at large value of the argument. χ_{FPT}^∞ is the skewness of the FPT distribution for large rod lengths. It is close to zero for almost all the temperatures. The exponent (γ) of the power law turns out to be not universal across different models. So we plotted the data as a function of $(\xi_{rod}^S/L_{rod})^\gamma$ to collapse all the data in one master curve. The collapse and the power law seems reasonably good, suggesting that $\chi_{FPT} \sim (\xi_{rod}^S)^\gamma$ is probably robust across different systems. The value of the exponent γ is 1.5 for both 3dKA and 2dMKA model and 3.0 for 3dHP model. A detailed understanding of this relation and the value of the exponent is lacking at this moment. Thus if one can extract the exponent, γ for supercooled glycerol, then one might be able to even directly compute the growth of the static length scale without performing the scaling analysis. Nevertheless, this scaling relation does suggest that skewness of the FPT distribution is a direct measure of static correlation in supercooled liquids. Although at this moment, we are not able to estimate the growth of amorphous order in supercooled glycerol due to lack of experimental data at different length of the probe molecules in supercooled glycerol, but we have clearly demonstrated the generality and the strength of the proposed methodology for measuring the growth of static correlation in experimentally studied glass-forming liquids.

CONCLUSIONS

To conclude, we have studied the dynamics of rod-like particles in supercooled liquid medium with varying lengths of the rods. We showed that rotational motions of the rod start to show non-normal behaviour once the host medium is in supercooled regime. By analyzing the variation of non-normal measure with increasing rod length at timescales equal to the α -relaxation time of the supercooled liquid, we are able to obtain the dynamic heterogeneity length scale of the liquid at that instance of time. We then showed that the distribution of the relaxation time or the first passage time of the rod in our simulation studies are

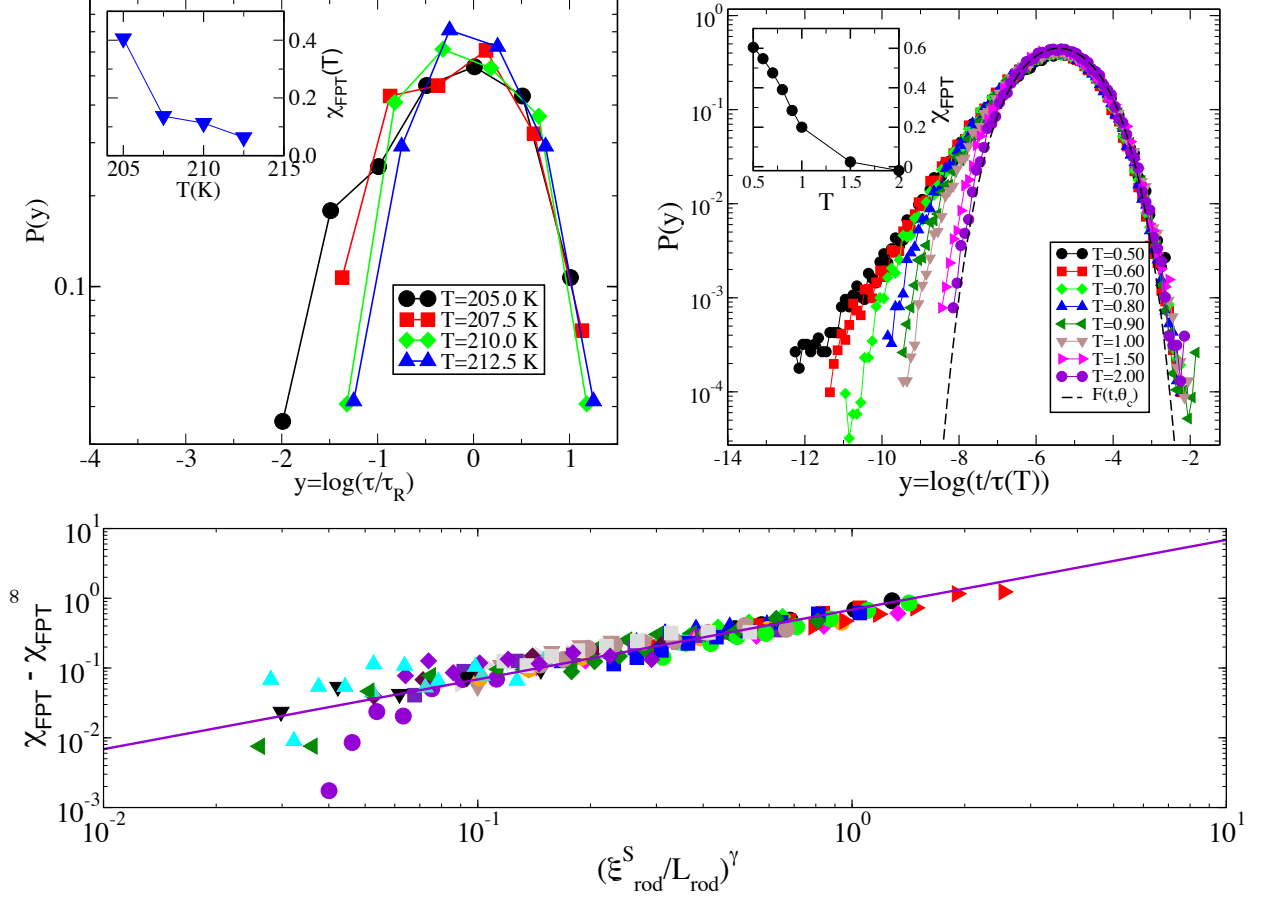


FIG. 5. Top Left panel: Distribution of correlation time of Dye molecules in supercooled glycerol for four different temperatures. Data is taken from Ref.[40]. The distribution is rescaled by the mean correlation time. Note the clear signature of short time shoulder in the distribution at lower temperatures. Inset shows the skewness of the distributions. Top Right panel: Distribution of first passage time for a rod of length 2.8 embedded in 3dKA model for various temperatures. These distributions also show the development of shoulder (excess wing) in the distribution at lower temperatures. The dashed line in through the data points is the best fit to Eq.8. The inset shows the skewness of the distribution. The similarity between experimental data and simulation results are very striking. Bottom panel: Shows the skewness, χ_{FPT} for all the three model systems plotted as $(\xi_{rod}^S/L_{rod})^\gamma$ with $\gamma = 1.5$ for 3dKA and 2dmKA models and $\gamma = 3.0$ for 3dHP model respectively. The nice scaling collapse suggests that $\chi_{FPT} \sim (\xi_{rod}^S)^\gamma$ for a given rod length at large value of ξ_{rod}^S . See discussion in the text.

in complete agreement with experimental results obtained using gold nano-rods and other elongated rod-like dye molecules in supercooled glycerol. Our complete statistical analysis of the first passage time distribution of the rod shows that the problem can be exactly mapped into a Brownian motion of the rod with two absorbing boundary conditions. The asymptotic form of the distribution obtained from the exact results for a Brownian particle with two absorbing boundary condition shows remarkable match with the obtained distribution of the first passage time from simulations for all the studied glass-forming model liquids. Our results thus also establish that the distribution of rotational relaxation time in experiments is not log-normal rather has a completely different form which can be analytically obtained by solving the equation of motion of Brownian rod with two absorbing boundary conditions. In the experimental works it was claimed that increasing width of the relaxation time of the rod is a direct indicator of the growing dynamic heterogeneity in the system, but it was not clear how to obtain the underlying length scale from these results. Our results suggest that to quantitatively obtain the dynamic heterogeneity length scale and the static length scale, one needs to extend these experimental studies by systematically changing the length of probe molecules. Thus we think that dynamics of rod-like probe molecule in supercooled liquid is an interesting and novel way to extract various length scales of importance in glass-forming liquids and the method is clearly accessible for experimentally relevant glass forming liquids. We thus hope that our study will encourage experimentalists to extend their single molecule probe experiments in supercooled liquids to extract the dynamical heterogeneity length and the static length in these systems.

METHOD SECTION

We have done NPT simulations for all of the three models studied. We refer these models as: **3dKA Model**, **3dHP Model** and **2dmKA Model** respectively. Details of these models can be found in the SI. 3dKA model is the well-known 80:20 binary mixture of A and B type interacting via Lennard-Jones pairwise potential[45]. 3dHP model [46] is a bridge between the finite-temperature glasses and hard-sphere glasses and is usually studied in context of jamming. It is a 50:50 binary mixture of soft spheres with diameter ratio 1.4 and interacting via harmonic pair potential. 2dmKA model [47] is a modified version of 3dKA model in two dimensions. It is 65:35 binary mixture. The temperature and pressure in the simulation is controlled by Brendsen thermostat and barostat [48]. A different thermostat does not change the results qualitatively.

In all of the glass formers mentioned above we have added few (two in 3dKA and one in 3dHP, 2dmKA) rigid rods made up of variable number of spheres N , each separated by a fixed distance from the other by a distance of $0.3\sigma_{AA}$, where σ_{AA} is the diameter of the largest particle type (A) for 3dKA and 2dmKA models. For 3dHP model we used $0.42\sigma_{AA}$. Each of the sphere in a rod have same mass and interacts via same potential as particles in the host liquid. The rod length is defined as $L = 0.3 * (N - 1) + 1.0$ for 3dKA and 2dmKA models and $L = 0.42 * (N - 1) + 1.0$ for 3dHP model. See SI for further details. Equation of motion for translational dynamics of spheres and center of mass (COM) of rods is integrated by usual Leap-Frog integrator. The dynamics of rod's orientation vector ($\hat{\mathbf{u}}$) is also integrated by the same integrator but strictly following the methods illustrated in [48, 49].

Acknowledgements: We would like to thank Kabir Ramola and Bhanu Prasad Bhowmik for many useful discussions. We also like to acknowledge Vikash Pandey for his help in the initial part of the project. Authors are grateful to Satya Majumder for his comments and suggestions. We also thank Hajime Tanaka, Hajime Yoshino and Kunimasa Miyazaki for many useful discussion during the Beijing Meeting 2019. This project is funded by intramural funds at TIFR Hyderabad from the Department of Atomic Energy (DAE). Support from Swarna Jayanti Fellowship grants DST/SJF/PSA-01/2018-19 and SB/SFJ/2019-20/05 are also acknowledged.

-
- [1] M. D. Ediger, Spatially heterogeneous dynamics in supercooled liquids. *Annual Review of Physical Chemistry* **51**, 99-128 (2000). PMID: 11031277.
 - [2] L. Berthier, G. Biroli, Theoretical perspective on the glass transition and amorphous materials. *Reviews of Modern Physics* **83**, 587–645 (2011).
 - [3] A. S. Keys, A. R. Abate, S. C. Glotzer, D. J. Durian, Measurement of growing dynamical length scales and prediction of the jamming transition in a granular material. *Nature Physics* **3**, 260 EP - (2007).
 - [4] T. Kawasaki, H. Tanaka, Structural origin of dynamic heterogeneity in three-dimensional colloidal glass formers and its link to crystal nucleation. *Journal of Physics: Condensed Matter* **22**, 232102 (2010).
 - [5] T. Kawasaki, T. Araki, H. Tanaka, Correlation between dynamic heterogeneity and medium-range order in two-dimensional glass-forming liquids. *Phys. Rev. Lett.* **99**, 215701 (2007).
 - [6] R. Richert, Heterogeneous dynamics in liquids: fluctuations in space and time. *Journal of Physics: Condensed Matter* **14**, R703–R738 (2002).
 - [7] D. N. Perera, P. Harrowell, Relaxation dynamics and their spatial distribution in a two-dimensional glass-forming mixture. *The Journal of Chemical Physics* **111**, 5441–5454 (1999).
 - [8] P. Chaudhuri, L. Berthier, W. Kob, Universal nature of particle displacements close to glass and jamming transitions. *Phys. Rev. Lett.* **99**, 060604 (2007).
 - [9] S. Karmakar, C. Dasgupta, S. Sastry, Growing length and time scales in glass-forming liquids. *Proceedings of the National Academy of Sciences* **106**, 3675–3679 (2009).
 - [10] S. Karmakar, C. Dasgupta, S. Sastry, Growing length scales and their relation to timescales in glass-forming liquids. *Annual Review of Condensed Matter Physics* **5**, 255-284 (2014).
 - [11] S. Karmakar, C. Dasgupta, S. Sastry, Length scales in glass-forming liquids and related systems: a review. *Reports on Progress in Physics* **79**, 016601 (2015).
 - [12] T. R. Kirkpatrick, D. Thirumalai, P. G. Wolynes, Scaling concepts for the dynamics of viscous liquids near an ideal glassy state. *Phys. Rev. A* **40**, 1045–1054 (1989).
 - [13] V. Lubchenko, P. G. Wolynes, Theory of structural glasses and supercooled liquids. *Annual Review of Physical Chemistry* **58**, 235-266 (2007).
 - [14] G. Biroli, J.-P. Bouchaud, A. Cavagna, T. S. Grigera, P. Verrocchio, Thermodynamic signature of growing amorphous order in glass-forming liquids. *Nature Physics* **4**, 771-775 (2008).
 - [15] G. Biroli, S. Karmakar, I. Procaccia, Comparison of static length scales characterizing the glass transition. *Phys. Rev. Lett.* **111**, 165701 (2013).
 - [16] S. Karmakar, E. Lerner, I. Procaccia, Direct estimate of the static length-scale accompanying the glass transition. *Physica A: Statistical Mechanics and its Applications* **391**, 1001–1008 (2012).

- [17] W. Kob, S. Roldán-Vargas, L. Berthier, Non-monotonic temperature evolution of dynamic correlations in glass-forming liquids. *Nature Physics* **8**, 164–167 (2011).
- [18] I. Tah, S. Sengupta, S. Sastry, C. Dasgupta, S. Karmakar, Glass transition in supercooled liquids with medium-range crystalline order. *Phys. Rev. Lett.* **121**, 085703 (2018).
- [19] R. Das, I. Tah, S. Karmakar, Possible universal relation between short time β -relaxation and long time α -relaxation in glass-forming liquids. *The Journal of Chemical Physics* **149**, 024501 (2018).
- [20] H. Tanaka, H. Tong, R. Shi, J. Russo, Revealing key structural features hidden in liquids and glasses. *Nature Reviews Physics* **1**, 333–348 (2019).
- [21] C. Patrick Royall, S. R. Williams, T. Ohtsuka, H. Tanaka, Direct observation of a local structural mechanism for dynamic arrest. *Nature Materials* **7**, 556–561 (2008).
- [22] L. Berthier, G. Biroli, J.-P. Bouchaud, L. Cipelletti, W. van Saarloos, eds., *Dynamical Heterogeneities in Glasses, Colloids, and Granular Media* (Oxford University Press, 2011).
- [23] C. Dasgupta, A. V. Indrani, S. Ramaswamy, M. K. Phani, Is there a growing correlation length near the glass transition? *Europhysics Letters (EPL)* **15**, 307–312 (1991).
- [24] C. Donati, S. C. Glotzer, P. H. Poole, Growing spatial correlations of particle displacements in a simulated liquid on cooling toward the glass transition. *Phys. Rev. Lett.* **82**, 5064–5067 (1999).
- [25] P. H. Poole, C. Donati, S. C. Glotzer, Spatial correlations of particle displacements in a glass-forming liquid. *Physica A: Statistical Mechanics and its Applications* **261**, 51 - 59 (1998).
- [26] I. Tah, S. Karmakar, Signature of dynamical heterogeneity in spatial correlations of particle displacement and its temporal evolution in supercooled liquids (2019).
- [27] B. P. Bhowmik, I. Tah, S. Karmakar, Non-gaussianity of the van hove function and dynamic-heterogeneity length scale. *Physical Review E* **98** (2018).
- [28] S. Chakrabarty, I. Tah, S. Karmakar, C. Dasgupta, Block analysis for the calculation of dynamic and static length scales in glass-forming liquids. *Phys. Rev. Lett.* **119**, 205502 (2017).
- [29] E. R. Weeks, Three-dimensional direct imaging of structural relaxation near the colloidal glass transition. *Science* **287**, 627–631 (2000).
- [30] W. K. Kegel, Direct observation of dynamical heterogeneities in colloidal hard-sphere suspensions. *Science* **287**, 290–293 (2000).
- [31] Y. Rahmani, K. van der Vaart, B. van Dam, Z. Hu, V. Chikkadi, P. Schall, Dynamic heterogeneity in hard and soft sphere colloidal glasses. *Soft Matter* **8**, 4264 (2012).
- [32] D. Bonn, W. K. Kegel, Stokes–einstein relations and the fluctuation-dissipation theorem in a supercooled colloidal fluid. *The Journal of Chemical Physics* **118**, 2005–2009 (2003).
- [33] C. K. Mishra, A. Rangarajan, R. Ganapathy, Two-step glass transition induced by attractive interactions in quasi-two-dimensional suspensions of ellipsoidal particles. *Physical Review Letters* **110** (2013).
- [34] L. Berthier, Direct experimental evidence of a growing length scale accompanying the glass transition. *Science* **310**, 1797–1800 (2005).
- [35] L. Berthier, G. Biroli, J.-P. Bouchaud, W. Kob, K. Miyazaki, D. R. Reichman, Spontaneous and induced dynamic fluctuations in glass formers. i. general results and dependence on ensemble and dynamics. *The Journal of Chemical Physics* **126**, 184503 (2007).
- [36] L. Berthier, G. Biroli, J.-P. Bouchaud, W. Kob, K. Miyazaki, D. R. Reichman, Spontaneous and induced dynamic correlations in glass formers. ii. model calculations and comparison to numerical simulations. *The Journal of Chemical Physics* **126**, 184504 (2007).
- [37] G. Biroli, J.-P. Bouchaud, K. Miyazaki, D. R. Reichman, Inhomogeneous mode-coupling theory and growing dynamic length in supercooled liquids. *Phys. Rev. Lett.* **97**, 195701 (2006).
- [38] S. Albert, T. Bauer, M. Michl, G. Biroli, J.-P. Bouchaud, A. Loidl, P. Lunkenheimer, R. Tourbot, C. Wiertel-Gasquet, F. Ladieu, Fifth-order susceptibility unveils growth of thermodynamic amorphous order in glass-formers. *Science* **352**, 1308–1311 (2016).
- [39] K. H. Nagamanasa, S. Gokhale, A. K. Sood, R. Ganapathy, Direct measurements of growing amorphous order and non-monotonic dynamic correlations in a colloidal glass-former. *Nature Physics* **11**, 403–408 (2015).
- [40] R. Zondervan, F. Kulzer, G. C. G. Berkhout, M. Orrit, Local viscosity of supercooled glycerol near T_g probed by rotational diffusion of ensembles and single dye molecules. *Proceedings of the National Academy of Sciences* **104**, 12628–12633 (2007).
- [41] H. Yuan, S. Khatua, P. Zijlstra, M. Orrit, Individual gold nanorods report on dynamical heterogeneity in supercooled glycerol. *Faraday Discussions* **167**, 515 (2013).
- [42] R. Jain, K. L. Sebastian, Diffusing diffusivity: Rotational diffusion in two and three dimensions. *The Journal of Chemical Physics* **146**, 214102 (2017).
- [43] V. Balakrishnan, *Mathematical Physics* (Springer International Publishing, 2020).
- [44] R. Das, S. Chakrabarty, S. Karmakar, Pinning susceptibility: a novel method to study growth of amorphous order in glass-forming liquids. *Soft Matter* **13**, 6929–6937 (2017).
- [45] W. Kob, H. C. Andersen, Testing mode-coupling theory for a supercooled binary lennard-jones mixture i: The van hove correlation function. *Phys. Rev. E* **51**, 4626–4641 (1995).
- [46] C. S. O’Hern, S. A. Langer, A. J. Liu, S. R. Nagel, Random packings of frictionless particles. *Phys. Rev. Lett.* **88**, 075507 (2002).
- [47] R. Brüning, D. A. St-Onge, S. Patterson, W. Kob, Glass transitions in one-, two-, three-, and four-dimensional binary lennard-jones systems. *Journal of Physics: Condensed Matter* **21**, 035117 (2008).
- [48] M. P. Allen, D. J. Tildesley, *Computer Simulation of Liquids* (Clarendon Press, New York, NY, USA, 1989).
- [49] D. C. Rapaport, *The Art of Molecular Dynamics Simulation* (Cambridge University Press, 2004).

Supplementary Information:
Dynamics of Rod like Particles in Supercooled Liquids - Probing Dynamic Heterogeneity and Amorphous Order

Anoop Mutneja* and Smarajit Karmakar†
*Tata Institute of Fundamental Research, 36/P, Gopanpally Village,
Serilingampally Mandal, Ranga Reddy District, Hyderabad, 500107, Telangana, India*

* anoopm@tifrh.res.in
† smarajit@tifrh.res.in

I. DEFINITIONS/METHODS

A. van Hove Function

The van Hove Function is defined as probability density of finding a particle ‘ i ’ in the vicinity of \mathbf{r} at time t , knowing that particle ‘ j ’ was in the vicinity of origin at time $t = 0$.

$$G(\mathbf{r}, t) = \frac{1}{N} \left\langle \sum_{i=1}^N \sum_{j=1}^N \delta(\mathbf{r} - (\mathbf{r}_i(t) - \mathbf{r}_j(0))) \right\rangle \quad (1)$$

The van Hove Function is usually decomposed into self part, $G_s(\mathbf{r}, t)$ and distinct part, $G_d(\mathbf{r}, t)$. Self part is defined as the probability density of finding particle ‘ i ’ in the vicinity of \mathbf{r} at time t , while knowing that it was in vicinity of origin at time $t = 0$.

$$G_s(\mathbf{r}, t) = \frac{1}{N} \left\langle \sum_{i=1}^N \delta(\mathbf{r} - (\mathbf{r}_i(t) - \mathbf{r}_i(0))) \right\rangle \quad (2)$$

Distinct part of van Hove function is defined by considering different i and j particles in Eq:1. Self part can also be thought as fraction of particles reaching in the vicinity of \mathbf{r} at time ‘ t ’ while all starting from origin (displacement distribution function). If particles follow normal diffusive dynamics in isotropic medium then in the limit of large time and displacement self part of van Hove function is given by

$$G_s(\mathbf{r}, t) \xrightarrow{t, r \rightarrow \infty} \frac{1}{(4\pi Dt)^{3/2}} \exp\left(-\frac{r^2}{4Dt}\right) \quad (3)$$

This expression is true for a Brownian particle in homogeneous medium at all times. Thus Non-Gaussianity of self part of van Hove function is a good measure for heterogeneity in the system at different times, where heterogeneity is meant by spatial variation of diffusion constant. Thus, non-Gaussian parameter, $\alpha_2(t)$ becomes the obvious choice to measure dynamic heterogeneity in a disordered system.

$$\alpha_2(t) = 1 - \frac{\langle |\mathbf{r}|^4 \rangle}{3 \langle |\mathbf{r}|^2 \rangle^2} \quad (4)$$

B. Four-Point Susceptibility $\chi_4(t)$

Four-Point Susceptibility [1, 2] is calculated as the variance or fluctuation of two point density correlation function or the overlap function $Q(t)$. Overlap function gives the measure of overlap between two configuration separated by time interval ‘ t ’ and is defined as follows:

$$Q(t) = \sum_{i=1}^N \theta(a - |\mathbf{r}_i(t) - \mathbf{r}_i(0)|) \quad (5)$$

where $\theta(x)$ is the usual step function and value of a is chosen to ignore the decorrelation that might happen due to vibrational motion of particles in their cages. Thus the variance of overlap function ($\chi_4(t)$) at time t will be the measure of fluctuation in relaxation in the system at that particular time due to dynamic heterogeneity. It is defined as

$$\chi_4(t) = \frac{1}{N} \left[\langle Q^2(t) \rangle - \langle Q(t) \rangle^2 \right] \quad (6)$$

Structural relaxation time τ_α is also defined in terms of overlap function, it is the time when average value of overlap function reduces to $1/e$ i.e. $\langle Q(\tau_\alpha) \rangle = 1/e$. Note that the temperature dependence of τ_α doesn’t depend on the chosen value of a .

C. Point-to-Set Method

The existence of Mosaic state and a static length scale is proposed in RFOT theory. It is theoretically proposed that the static length scale can be measured using a special correlation function, termed as the Point-to-Set (PTS) correlation function [3].

The length scale obtained from the analysis of PTS correlation function is generally called PTS length scale. A full theoretical consideration can be found in reference [3]. PTS length scale (ξ_{PTS}) is calculated by taking a well equilibrated configuration of the system and then freezing all the particles outside a region \mathcal{C} of linear dimension ξ as a boundary condition. The particles inside \mathcal{C} are then relaxed and overlap with the initial configuration is calculated. For small enough ξ overlap should be perfect implying that the particles inside are restricted to the same equilibrium state. With increasing ξ this overlap would vanish since particles inside would now explore more metastable states. The largest linear length scale $\xi = \xi_{PTS}$ to which volume of particles can be restricted to same metastable minimum is known as PTS length scale. Physically, it implies that mosaic of this linear dimension can survive in particular metastable state, and thus whole system can be thought of as divided into such mosaics of metastable states. The length scale obtained in this way is same as static length scale obtained by finite size scaling of τ_α and from minimum eigenvalue of Hessian matrix [4].

II. ROTATIONAL DYNAMICS OF ROD LIKE PARTICLES IN LIQUID

Two dimensional (2D) case: Rotational dynamics of rod in 2D is described by rotational diffusion equation for distribution density $\rho(\phi, t)$,

$$\frac{\partial \rho(\phi, t)}{\partial t} = D \frac{\partial^2}{\partial \phi^2} \rho(\phi, t) \quad (7)$$

where, $\phi \in [-\pi, \pi]$ is the polar angle with which rod is inclined to x- axis and D is the rotational diffusion coefficient. With appropriate boundary condition and rod along x-axis as a initial condition, one can obtain the following solution,

$$\rho(\phi, t) = \frac{1}{2\pi} + \frac{1}{\pi} \sum_{m=1}^{\infty} \cos(m\phi) e^{-m^2 Dt}. \quad (8)$$

The distribution density $\rho(\phi, t)$ is the self part of rotational van Hove function (Eq:2) for Brownian rods in homogeneous medium and with this solution the rotational mean square displacement (RMSD) and the non-normal parameter for rod dynamics can be calculated. Note that $\langle \cos\phi \rangle = e^{-Dt}$ and $\langle \cos 2\phi \rangle = e^{-4Dt}$ so the RMSD would be,

$$\begin{aligned} RMSD(t) &= \langle |\hat{u}(t) - \hat{u}(0)|^2 \rangle = 2(1 - \langle \cos\phi \rangle) \\ &= 2(1 - e^{-Dt}) \end{aligned} \quad (9)$$

where $\hat{u}(t)$ is the orientation vector of rod at time t . This expression for RMSD (Eq:10) can be used to fit simulation results to extract the value of rotational diffusion constant of rod. Next, in the spirit of finding the non-normal parameter for rotational distribution density of rods just like binder cumulant, *Jain et. al.* [5] shows that $\alpha_{rot,2D}(t)$ (Eq:11) is zero for $P(\phi, t)$ which can be verified by just using the above averaged values.

$$\begin{aligned} \alpha_{rot,2D} &= \frac{1}{3} \frac{\langle |\hat{u}(t) - \hat{u}_0|^4 \rangle}{(\langle |\hat{u}(t) - \hat{u}_0|^2 \rangle)^2} - \frac{1}{24} \frac{\langle |\hat{u}(t) - \hat{u}_0|^2 \rangle}{\langle |\hat{u}(t) - \hat{u}_0|^2 \rangle - 8} - 1 \\ &\times (\langle |\hat{u}(t) - \hat{u}_0|^2 \rangle - 8) - 1 \end{aligned} \quad (11)$$

Non-zero value of this parameter at time t would signify the fluctuation in rotational diffusion constant at that time. Thus we have used this parameter in main text to quantify dynamic heterogeneity at the length scale of rod.

Three dimensional (3D) case: The rotational diffusion equation in three dimensions reads out,

$$\frac{\partial \rho(\theta, \phi, t)}{\partial t} = -D \mathcal{R}^2 \rho(\theta, \phi, t) \quad (12)$$

where $\theta \in [0, \pi]$, $\phi \in [0, 2\pi]$ is azimuthal angle and polar angle subtended by the rod and D is diffusion constant. The rotational operator \mathcal{R}^2 is defined as

$$\mathcal{R}^2 = - \left\{ \frac{1}{\sin\theta} \frac{\partial}{\partial \theta} \left(\sin\theta \frac{\partial}{\partial \theta} \right) + \frac{1}{\sin^2\theta} \frac{\partial^2}{\partial \phi^2} \right\} \quad (13)$$

Solution to this equation with relevant boundary conditions can be obtained by introducing the spherical harmonics with the initial condition of rod to be along +ve z-axis, we can integrate out ϕ to get the solution,

$$\rho(\theta, t) = \sum_{n=0}^{\infty} \frac{2n+1}{2} P_n(\cos(\theta)) e^{-n(n+1)Dt} \quad (14)$$

where $P_n(\cos(\theta))$ is the Legendre polynomial of degree n . The average of any function $A(\theta)$ can be calculated as

$$\langle A(\theta) \rangle = \int_0^\pi d\theta \sin\theta A(\theta) \rho(\theta, t). \quad (15)$$

Like in 2D, $\langle \cos\theta \rangle$ and $\langle \cos 2\theta \rangle$ can be calculated easily and they are e^{-2Dt} and $\frac{1}{3}(4e^{-6Dt} - 1)$ respectively. So the rotational mean square displacement and the non-normal parameter[5] in 3D turn out to be,

$$\langle |\hat{u}(t) - \hat{u}(0)|^2 \rangle = 2(1 - \langle \cos\theta \rangle) = 2(1 - e^{-2Dt}) \quad (16)$$

$$\alpha_{rot,3D} = \frac{1}{2} \frac{\langle |\hat{u}(t) - \hat{u}_0|^4 \rangle}{(\langle |\hat{u}(t) - \hat{u}_0|^2 \rangle)^2} + \frac{1}{6} \langle |\hat{u}(t) - \hat{u}_0|^2 \rangle - 1 \quad (17)$$

III. ROTATIONAL MEAN SQUARED DISPLACEMENT(RMSD)

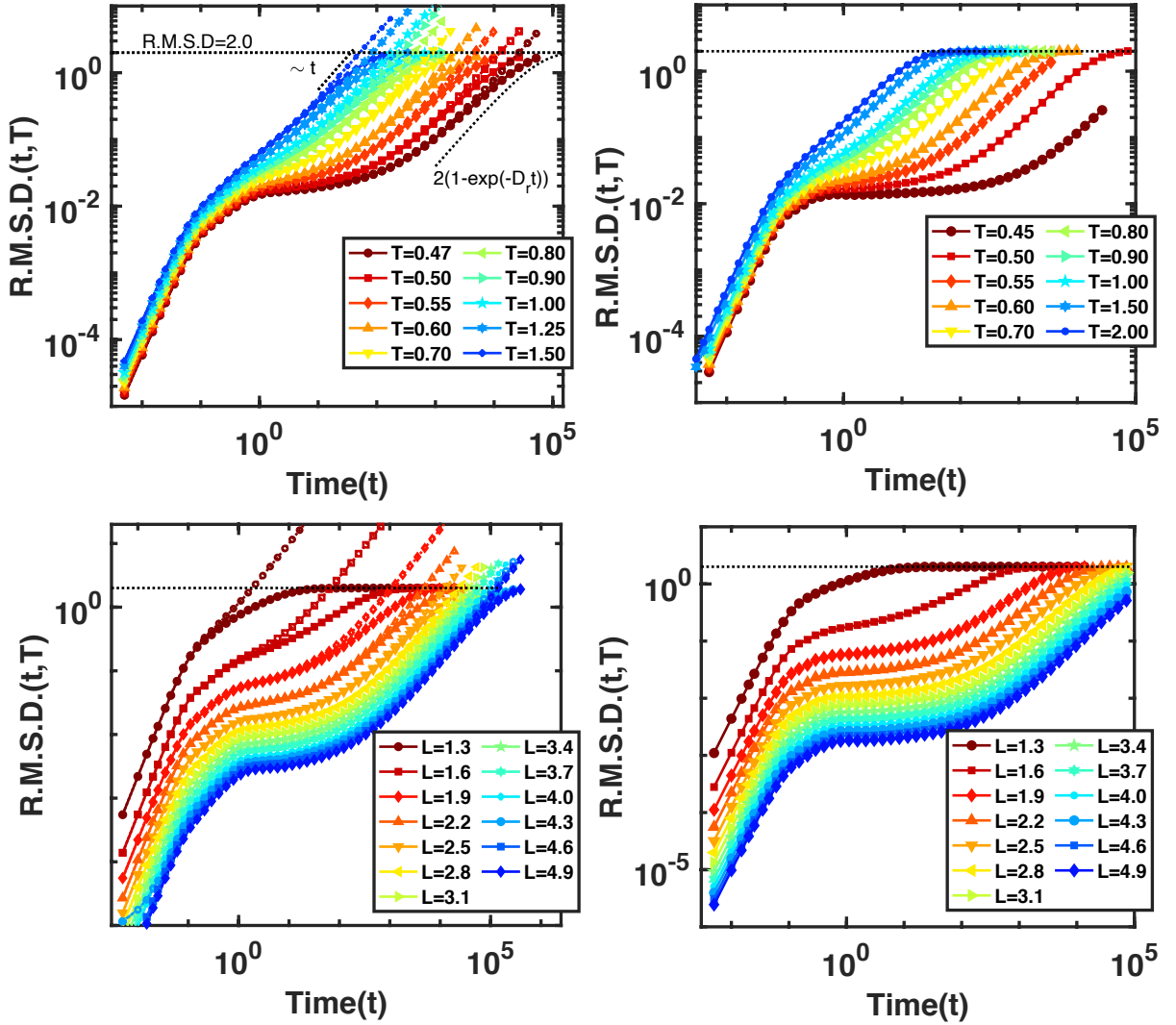


FIG. 1. Top panel: Time evolution of RMSD for rod of length $L = 2.5$ ($N = 6$ beads) immersed in 2dMKA (left) and 3dKA (right) model systems at various temperatures. Bottom panel: Time evolution of RMSD for rod of different lengths immersed in 2dMKA (left) and 3dKA (right) model systems at $T = 0.5$ temperature. Dotted lines in the plots 2dMKA model (left) are RMSD plots in the unfolded coordinates

RMSD for orientation vector of rod ($\hat{\mathbf{u}}$) is simply given by,

$$RMSD = \langle |\hat{\mathbf{u}}(t) - \hat{\mathbf{u}}_0|^2 \rangle = 2(1 - \langle \hat{\mathbf{u}}(t) \cdot \hat{\mathbf{u}}_0 \rangle) \quad (18)$$

where $\hat{\mathbf{u}}(t)$ is the orientation vector of rod at time ' t ', $\hat{\mathbf{u}}_0$ is the initial orientation vector and angular bracket is for ensemble average. Fig:1 (top panel) is the time evolution plot of RMSD of rod (fixed length) immersed in 2dMKA (left) and 3dKA (right) model at different temperatures. In the left panel we have also plotted the RMSD in unfolded coordinates $\phi \in (-\infty, \infty)$ (dotted lines). One can clearly distinguish the ballistic, caging and diffusive regions and try to obtain rotational diffusion constant by fitting the diffusive region with exact expression Eq:10 & Eq:16 for 2D and 3D model respectively. The complete analysis of rotational diffusion constant is done later in this document. Similarly, Fig:1 (bottom panel) is RMSD evolution plot for rods of various lengths immersed in 2dMKA model (left) and 3dKA model (right) both kept at temperature $T = 0.50$. Plots for 3dHP model are similar and are not shown in this document.

Next we ask about the possible scaling function $B(L_{rod})$ of RMSD evolution plots with rod length in $RMSD(L_{rod}, T, t) = A(T)B(L_{rod})C(t)$. It turns out that in the ballistic and caging regime, RMSD for rods can be scaled by inverse of moment of inertia of rod i.e. $B(L_{rod}) = (I(L_{rod}))^{-1}$ (see Fig: 3) and in the diffusive regime, the rotational diffusion constant $D_r(T, L_{rod})$ also falls as $1/I(L_{rod})$ with rod length. Below we give details of these scaling analysis.

A. Scaling of Ballistic region

Since ballistic region refers to small time region in which the rods are not undergoing any collision with other rods, implying the rotational displacement to be

$$\Delta\theta = \omega\Delta t \quad (19)$$

where ω is the angular velocity of rod at initial time. So averaged RMSD would be,

$$\langle \Delta\theta^2 \rangle = \langle \omega^2 \rangle \Delta t^2 \quad (20)$$

which gives us rotational drift coefficient $D_{rot}^{drift} = \langle \omega^2 \rangle$. Invoking equipartition theorem i.e. $\langle \omega^2 \rangle = fK_bT/I$ we get,

$$D_{rot}^{drift} = \frac{fK_bT}{I(L_{rod})} \quad (21)$$

where f is the rotational degrees of freedom, one in 2D and two in 3D. This argument completely explains the observed scaling in the ballistic regime.

B. Scaling of Caged region

Caged region refers to the time region during which the system particles exhibits vibrational motion. The caging RMSD value $\langle \Delta\theta^2 \rangle_c$ is half of the vibration amplitude. Now if we assume each small portion (dx) of rod feel harmonic force with same spring constant k from medium during this time interval, then we can imagine a picture like Fig:2. In this Figure, $F_T(x)$ is the transverse force acting on rod element dx at distance x from center of mass of rod. If θ is the angular displacement at any time t , then transverse force on the rod element would be, $F_T(x) = -kx\theta\cos\frac{\theta}{2}$ and net torque on rod would be,

$$\begin{aligned} \tau = I\ddot{\theta} &= 2 \int_0^{L/2} x' F_T(x') dx' \\ &= -k \left(2 \int_0^{L/2} x'^2 dx' \right) \theta \cos \frac{\theta}{2} \\ &= -\frac{kI}{\rho} \theta \cos \frac{\theta}{2} \end{aligned} \quad (22)$$

where ρ is the mass density of rod. Since caging θ is going to be small thus on expanding the cosine term and keeping upto θ^2 terms we get,

$$\ddot{\theta} = -\frac{k}{\rho} \theta + \mathcal{O}(\theta^3) \approx -k'\theta \quad (23)$$

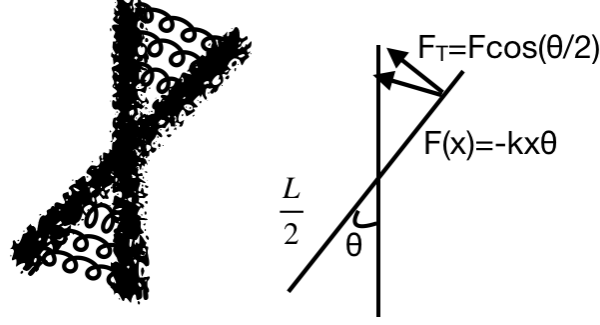


FIG. 2. Effective interaction picture of rod in caging regime.

where k' is now independent of rod length. This is the equation of simple harmonic motion (SHM) with solution $\theta(t) = \theta_0 \sin(\sqrt{k'}t)$ thus, $\langle \theta^2 \rangle = \langle \theta_0^2 \rangle / 2$. Also, the rotational mean squared velocity would be,

$$\langle \dot{\theta}^2 \rangle = k' \frac{\langle \theta_0^2 \rangle}{2}$$

and on using equipartition theorem we get,

$$\langle \theta^2 \rangle = \frac{\langle \dot{\theta}^2 \rangle}{k'} \sim \frac{f K_b T}{I(L_{rod})}$$

. Since we are modeling rods in a medium at constant pressure so as to maintain the same particle density at different temperatures, the time at which RMSD changes from ballistic to caging region should be independent of temperature. So, it is evident that one can get the master curve in ballistic and caging region for all temperatures if we scale the RMSD with $I(L_{rod})/T$, Fig:3 (right) is the master curve, where color code is for different rod lengths and different symbols are for different temperatures.

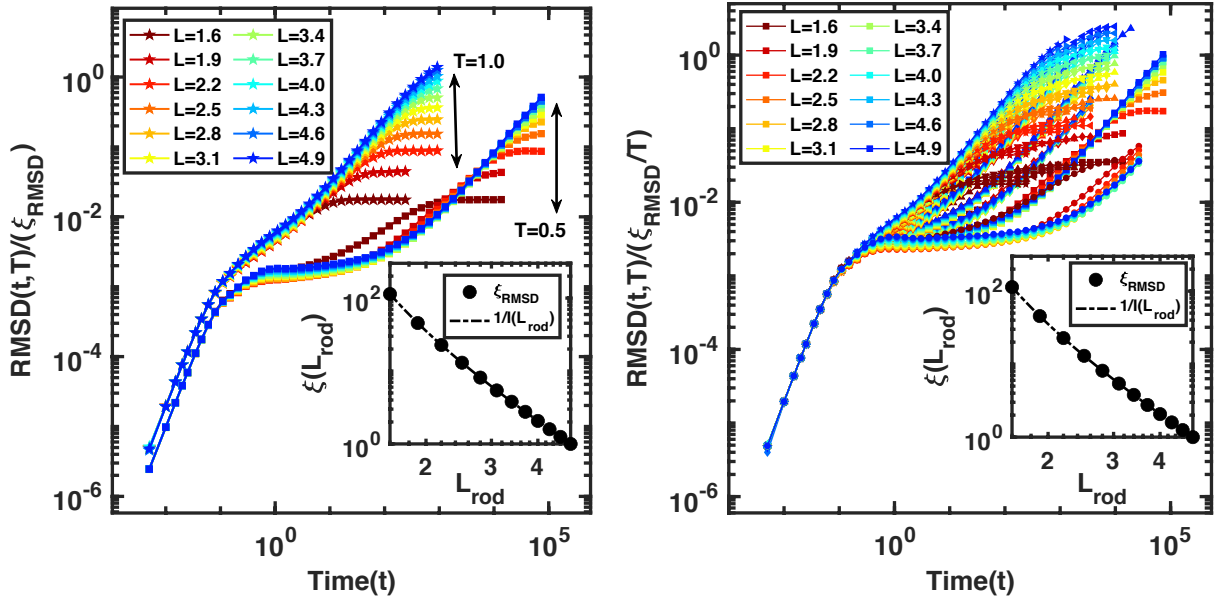


FIG. 3. Left panel: RMSD evolution plot scaled by $1/I(L_{rod})$ for rods of different length in 3dKA model liquid to get a collapse in ballistic and caging region. Right panel: Master curve of RMSD evolution plots obtained for rods of different lengths (different color) in systems at different temperature (different symbols) using a scaling function $T/I(L_{rod})$.

C. Diffusive regime

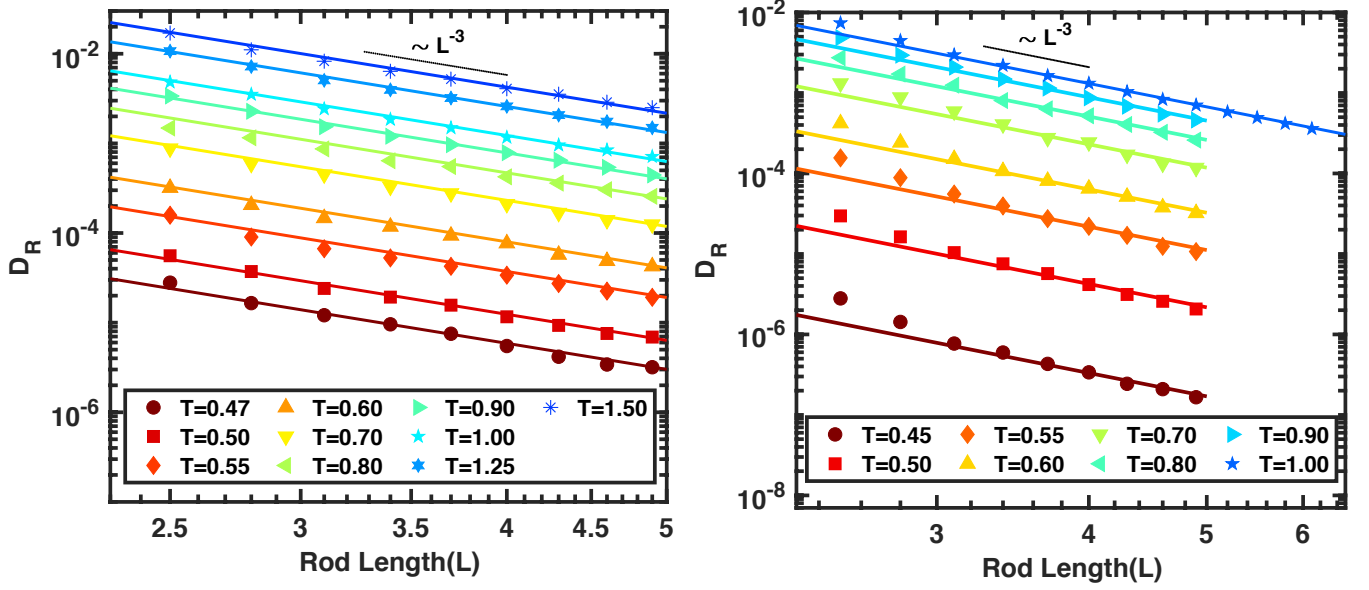


FIG. 4. Rod length variation of rotational diffusion constant of rod immersed in of 2DMKA system (left) and 3DKA system (right) system different temperatures. Solid lines in the plot are L^{-3} fit while symbols are actual values of $D_R(L)$ for rod of length L .

The Rotational diffusion constant can be calculated in the simulations by comparing the ensemble averaged value of $(\mathbf{u}(t) \cdot \mathbf{u}(0))$ with the exact expressions i.e. e^{-Dt} for 2D and e^{-2Dt} for 3D. Rod length dependence can also be obtained theoretically by considering the Langevin equation of motion for rods embedded in assembly of spheres. This will be a valid approximation for large rods. The Langevin equation reads out,

$$I \frac{d^2 \theta(t)}{dt^2} = -\zeta(L_{rod}) \frac{d\theta(t)}{dt} + \tau(t) \quad (24)$$

where $\theta = \cos^{-1}(\hat{\mathbf{u}}(t) \cdot \hat{\mathbf{u}}_0)$, $\zeta \dot{\theta}$ is the frictional torque and $\tau(t)$ is the rapidly fluctuating torque with $\langle \tau(t) \tau(t') \rangle = 2\zeta K_b T \delta(t - t')$. For large enough rods, the usual assumptions like θ independence of $\tau(t)$ and the large difference in the timescales of fluctuations in $\theta(t)$ and $\tau(t)$ are valid. So, on doing the standard calculation to obtain the rotational mean squared displacement one would get following expression for rotational diffusion constant,

$$D(L) = \frac{2K_b T}{\zeta(L)} \quad (25)$$

On assuming the rod to be a stack of beads (Shish-Kebab model) and each of which would experience the viscous force according to Stokes law, one can get the rod length scaling of $\zeta(L_{rod}) \sim I(L_{rod}) \sim L_{rod}^3$ (page no 291-293 of Ref:[6]). Hence, one gets the scaling for rotational diffusion constant to be $D_r \sim I(L_{rod})^{-1} \sim L_{rod}^{-3}$. Fig: 4 shows the variation of diffusion constant of rod with changing rod length when they are immersed in 2dMKA (left) and 3dKA (right) supercooled liquid at different temperature.

Another check for the scaling of $\zeta(L_{rod})$ would be to invoke fluctuation- dissipation theorem i.e.

$$\zeta(L_{rod}) = \frac{1}{K_b T} \int_0^\infty \langle \tau(t') \tau(t' + t) \rangle dt \quad (26)$$

and check for the rod length dependence of the integral. For delta correlated torques it is just the variance of the torque distribution on the rod. It has been checked and confirmed in simulations that the integral in the right side of above equation scales like L^3 for large rods. While this scaling doesn't hold for small rods which is not so difficult to understand because the Langevin approach would not work if size of Brownian particle is comparable to the liquid particle.

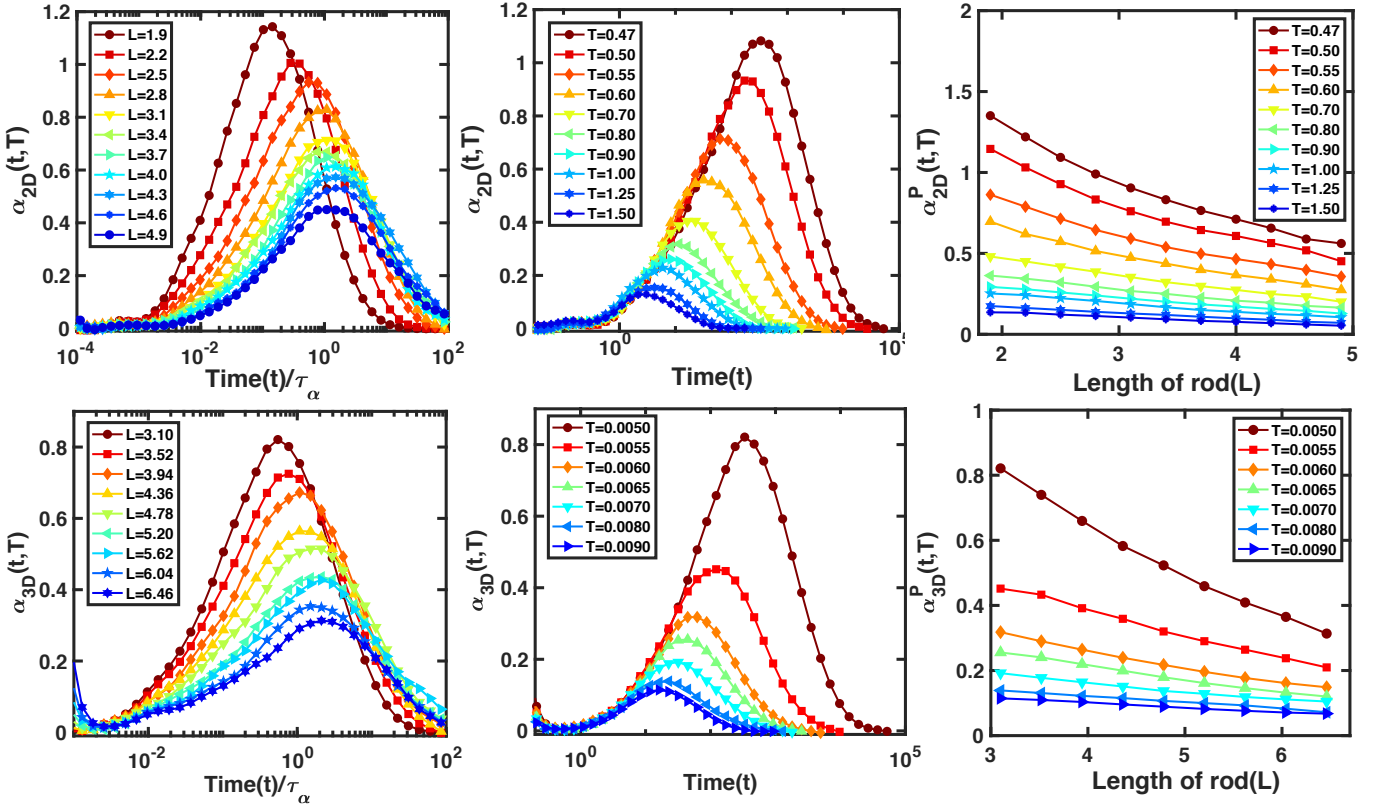


FIG. 5. Left panel: Evolution of non-normal parameter (α_{2d} or α_{3d}) for rod of different length immersed in 2dMKA (top) and 3dHP (bottom) model system at temperature $T = 0.5$ and $T = 0.0050$ respectively. Centre panel: Time evolution of α_{2d} or α_{3d} for rod of length $L_{rod} = 2.5$ and $L_{rod} = 3.10$ in model system 2dMKA (top) and 3dHP (bottom) respectively. Right panel: Rod length variation of peak value of NNP (α_{2d}^P or α_{3d}^P) for rod immersed in 2dMKA (top) and 3dHP (model) at various temperatures.

IV. NON-NORMAL PARAMETER AND DYNAMIC LENGTH SCALE

The Non-Normal parameter (NNP) [$\alpha_{rot2D}(t, T, L_{rod})$ & $\alpha_{rot3D}(t, T, L_{rod})$] is a measure of fluctuation in diffusion constant felt by rod at time t , immersed in a liquid at temperature T . As already pointed out NNP should be zero for rod immersed in homogeneous medium, so one should expect the same for rod in high temperature (or low density) liquid at all times and for all rod lengths. But in supercooled environment as shown in main text, this NNP would be non zero and will reach a maximum at time $t \sim \tau_\alpha$ similar to $\chi_4(t, T)$. Thus the peak height can be a good measure of dynamic heterogeneity and its increase with decreasing temperature confirms that. It is also shown that the peak height (α_{rot2D}^P & α_{rot3D}^P) decreases with increasing rod length because of rod seeing dynamical response of the surrounding medium averaged over the length scale of the rod. A length scale $\xi_{rod}(T)$ is obtained by scaling the rod length with an appropriate system length scale to obtain a master curve between $\alpha_{rot2D}^P(T)$ or $\alpha_{rot3D}^P(T)$ and $L_{rod}/\xi_{rod}(T)$. The collapse of $\alpha_{rot2D}^P(T)$ or $\alpha_{rot3D}^P(T)$ for all three model systems (3dKA, 3dHP and 2dMKA) are presented in main text and the length scales so obtained match very well with dynamic length scales obtained by traditional methods. The plots of time and rod-length variation of $\alpha_{rod2D}(T)$ or $\alpha_{rod3D}(T)$ at different temperatures for 3dKA model are given in main text, while Fig:5 contains same plots for 2dMKA (top panel) and 3dHP model (bottom panel).

V. ROTATIONAL CORRELATION FUNCTION

The l^{th} order orientation correlation function for 2D systems is defined as,

$$g_l(t) = \langle \cos[l\{\theta(t) - \theta(0)\}] \rangle$$

and for 3D systems it is defined as,

$$g_l(t) = \langle P_l(\cos[\theta(t)]) P_l(\cos[\theta(0)]) \rangle$$

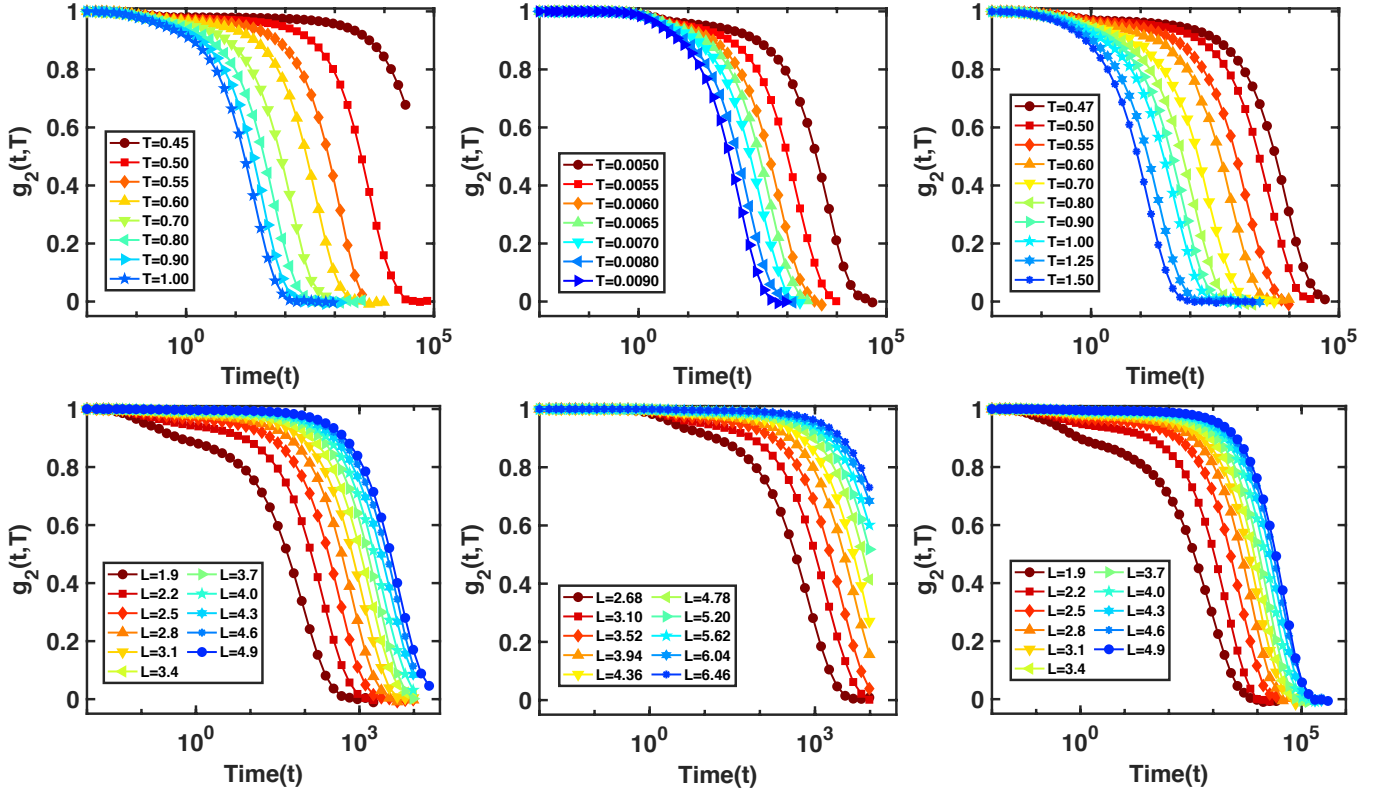


FIG. 6. Top panel: Second order orientation correlation function $g_2(t)$ for rod of length $L_{rod} = 2.5, 3.1 \& 2.5$ immersed in 3dKA, 3dHP & 2dmKA (left to right) model systems respectively at different temperatures. Bottom panel: Evolution of $g_2(t)$ for rod of various rod-length immersed in 3dKA, 3dHP & 2dmKA (left to right) model systems at temperatures $T = 0.60, 0.0055 \& 0.50$ respectively.

. Where P_l denotes the Legendre polynomial of l^{th} order. Both of them starts from $g_2 = 1$ at time $t = 0$ and approach zero in the limit of large time. Fig:6 are the rotational correlation functions for all three models. Fig:6 (top panel) shows the temperature variation of orientation correlation function of fixed length rod and Fig:6 (bottom panel) shows its rod length dependence for systems at fixed (low) temperature. Two step relaxation can be easily seen in these correlation function indicating again the effect of supercooling.

VI. FIRST PASSAGE TIME (FPT) DISTRIBUTION

As defined in the main text $F(t, \pm\phi_c)$ is distribution function for time when rod rotates by an angle $\phi = \pm\phi_c$ for the first time in 2D system while starting from $\phi = 0$. In the similar way $F(t, \theta_c)$ is the distribution function for time when rod touches the cone $\theta = \theta_c$ for the first time in 3D system while starting from $\theta = 0$. These can be calculated as a negative derivative of survival probabilities $S(t, \pm\phi_c)$ & $S(t, \theta_c)$, which are easy to get after solving for densities $\rho_c(t, \phi)$ and $\rho_c(t, \theta)$ in respective diffusion equation (Eq:7 for 2D and Eq: 12 for 3D) with appropriate boundary and initial conditions. In the following sections we present the solution for FPT distributions for 2D and 3D.

2D case: One can check that following is the solution of Eq:7 with two absorbing boundaries at $\phi = \pm\phi_c$ and $\phi = 0$ as initial condition.

$$\rho_c(\phi, t) = \frac{1}{\phi_c} \sum_{n=0}^{\infty} \cos\left(\frac{(2n+1)\pi\phi}{2\phi_c}\right) e^{-\frac{(2n+1)^2\pi^2}{4\phi_c^2}Dt} \quad (27)$$

Survival probability $S(t)$ can be calculated by integrating probability density $\rho_c(\phi, t)$ over whole ϕ space at time t , then a negative derivative with time would give the first passage distribution $F(t, \pm\phi_c)$.

$$S(t, \pm\phi_c) = \frac{4}{\pi} \sum_{n=0}^{\infty} \frac{(-1)^n}{(2n+1)} \exp\left(-\frac{(2n+1)^2\pi^2Dt}{4\phi_c^2}\right) \quad (28)$$

$$F(t, \pm\phi_c) = \frac{\pi D}{\phi_c^2} \sum_{n=0}^{\infty} (-1)^n (2n+1) \exp\left(-\frac{(2n+1)^2 \pi^2 D t}{(4\phi_c^2)}\right) \quad (29)$$

Fig:7 (top panel) shows the heat map of $\rho_c(\phi, t)$ (left) and the distribution $P(\log(t))$ (right) where t is first passage time. In the right panel we have also plotted $P(\log(t))$ obtained from Brownian dynamics simulation as outlined in the main text along with the exponential decay fit. Survival probability is also plotted in inset of right panel. In the main text we have argued the following approximate functional form for these FPT distributions.

$$F(t, \pm\phi_c) \propto t^{-\beta} e^{-\alpha/t} e^{-t/\tau} \quad (30)$$

Justification for this comes from small and large time limits of FPT distribution. Because of bounded space, it has to decay exponentially at large times (See Fig:7 top-left panel) which gives us third term and at small times it should be like normal Brownian motion which would provide us first two terms (for mathematical arguments refer to main text). In right panel of Fig:7 (top) we fitted above approximate function with actual solution, the fitting of function seems near perfect suggesting the correctness of approximate functional form of FPT distribution (Eq:30).

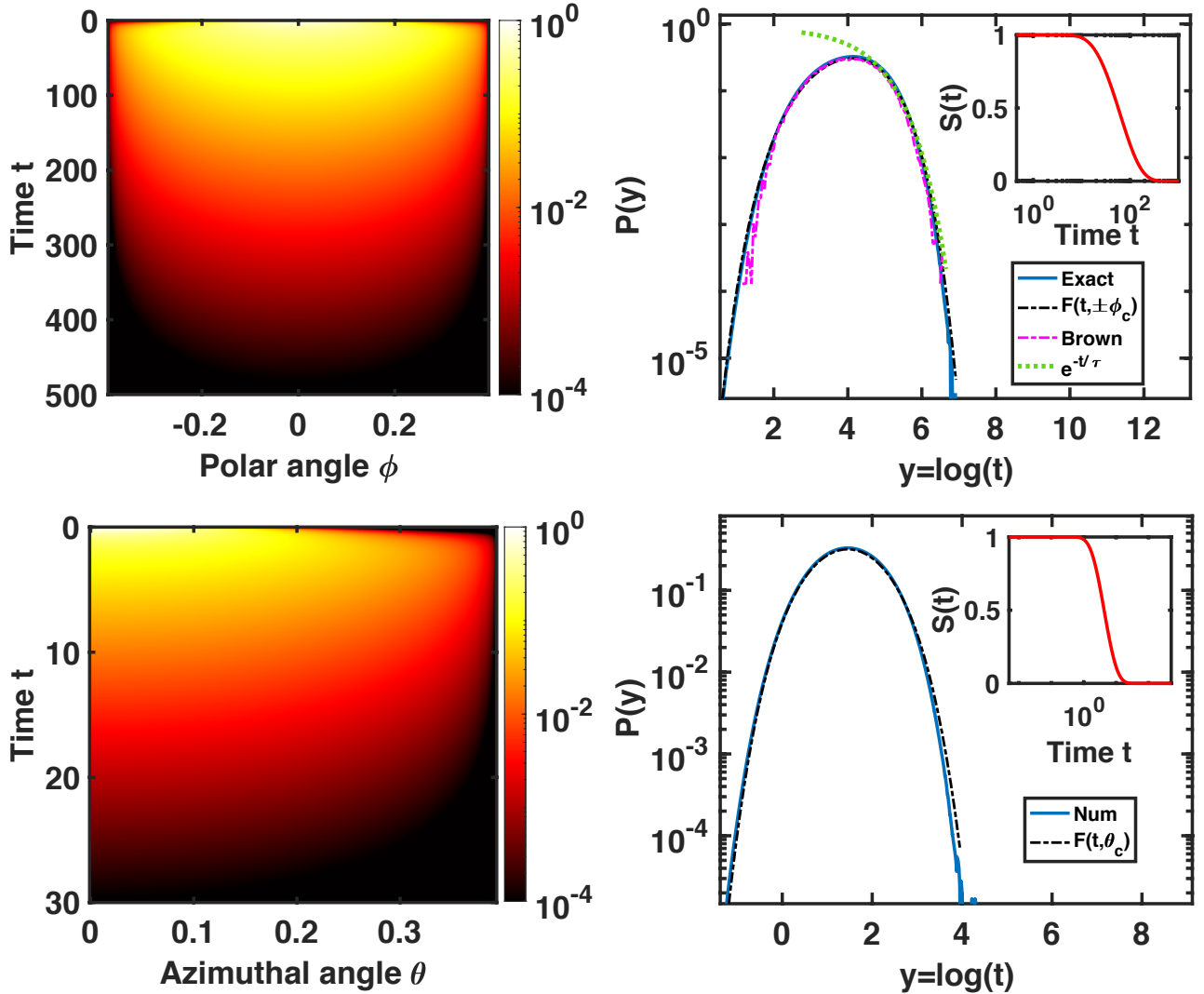


FIG. 7. Top panels: Heat-map (left) for $\rho_c(\phi, t)$ obtained by numerically integrating Eq:7 with absorbing boundaries at $\phi = \pm\phi_c$ and initial condition of $\phi = 0$. Right panel contains the FPT distribution $P(\log(t))$ fitted with proposed approximate function Eq:30, exponential decay function and Brownian dynamics result along with the survival probability $S(t)$ in the inset. Bottom panel: Same plots as top panel but for rod in 3D.

3D case: Unlike in 2D, getting solution of Eq:12 with absorbing cone at $\theta = \theta_c$ is not possible so we turn to numerical solution.

In Fig: 7 (bottom panel) we present the heat map (left) for $\rho_c(\theta, t)$ and the FPT distribution (right) $P(\log(t))$ with the inset of survival probability. The same approximate functional form Eq:30 also works for very well in 3D case.

In the main text it is mentioned that shape of the distribution $P(\log(t))$, doesn't changes with change in diffusion constant, only mean value of the distribution shifts by $-\log(D)$, this can be easily seen in case of 2D by writing $P(y)$ in a following form while in 3D it has been confirmed numerically,

$$\begin{aligned} P(y) &= \frac{\pi D e^y}{\phi_c^2} \sum_{n=0}^{\infty} (-1)^n (2n+1) \exp\left(-\frac{(2n+1)^2 \pi^2 D e^y}{(4\phi_c^2)}\right) \\ &= \frac{\pi e^{(y+\log D)}}{\phi_c^2} \sum_{n=0}^{\infty} (-1)^n (2n+1) \exp\left(-\frac{(2n+1)^2 \pi^2 e^{(y+\log D)}}{(4\phi_c^2)}\right) \end{aligned} \quad (31)$$

Thus, variance, skewness and all other higher order moments of distribution $P(\log(t))$ should be independent of $D(T, L_{rod})$ for homogeneous diffusion and hence independent of rod length and temperature. This becomes the reason of using $P(\log(t))$ to identify the structural changes (manifested in relaxation time) at the length scale of rod with increasing supercooling. Since diffusion constant $D(T, L_{rod}) \propto I(L_{rod})^{-1}$ for a rod of different length immersed in liquid at same temperature, the distribution $P(\log(t/I(L_{rod})))$ should be a master curve for that temperature. Thus, deviation from that master curve would be the measure of structural order at length scale of rod. In the main text Fig:3 are the distribution plots of $P(\log(t))$ and $P(\log(t/I(L_{rod})))$ for rod immersed in 3DKA model at different temperature. Same are plotted here for 2DMKA and 3DHP model in Fig:8. One can clearly see the effect of supercooling appearing in the form of short time shoulder for smaller rods. Thus, skewness of this distribution ($\chi_{FPT} = -\text{skewness}(P(\log(t)))$) qualifies best to capture the structural order at the length scale of rod. Collapse for χ_{FPT} is obtained by scaling the rod length with appropriate length scale ξ_{rod}^s to obtain master curve between $\chi_{FPT}(T, L_{rod})$ and L_{rod}/ξ_{rod}^s and is presented in main text for 3dKA, 3dHP and 2dmKA models. This obtained structural or static length scale matches well with the static length scale obtained using traditional methods like PTS method and finite size scaling of α -relaxation time. Since all experiments measuring the rotational diffusion of single probe molecule are done

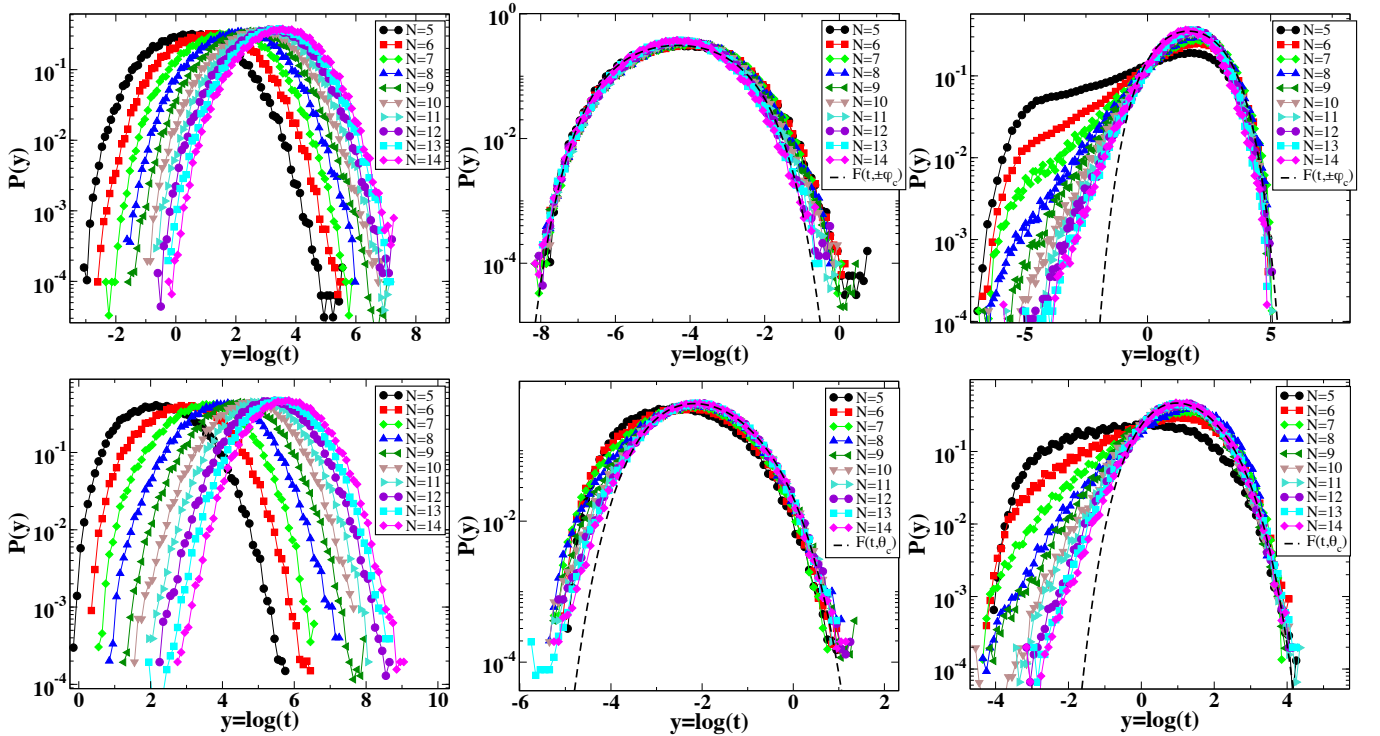


FIG. 8. Top panels: Distribution of unscaled (left) and scaled (center and right) first passage times for rods of various lengths in 2dMKA system at temperature $T = 1.5$ (high temperature) (left and center) and $T = 0.5$ (low temperature) (right) with absorbing boundary at $\theta_c = \pi/8$. Bottom panels: Distribution of unscaled (left) and scaled (center and right) first passage times for rods of various lengths in 3dHP system at temperature $T = 0.0090$ (high temperature) (left and center) and $T = 0.0050$ (low temperature) (right) with absorbing boundary at $\theta_c = \pi/8$.

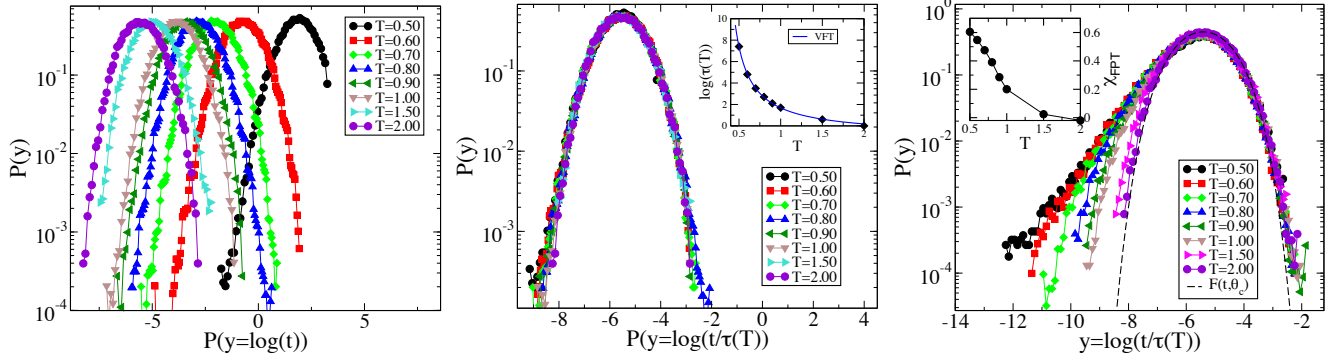


FIG. 9. Left & center panel: Distribution plots of $\log(t)$ where t is FPT for rod length $L_{rod} = 4.9$ in 3dKA system at different temperatures (left) and $P(\log(t/\tau(T)))$ where $\tau(T)$ is chosen to obtain master curve (center). In the inset of center panel $\tau(T)$ is plotted along with the Vogel-Fulcher-Tammann (VFT) fit. Right panel: Distribution of $\log(t/\tau(T))$ for rod of length $L_{rod} = 2.8$ in 3dKA system at different temperatures, here $\tau(T)$ is same to that of $L_{rod} = 4.9$ case chosen to subtract the obvious temperature scaling. In the inset χ_{FPT} is plotted to depict growing structural correlation at the length scale of rod with decreasing temperature.

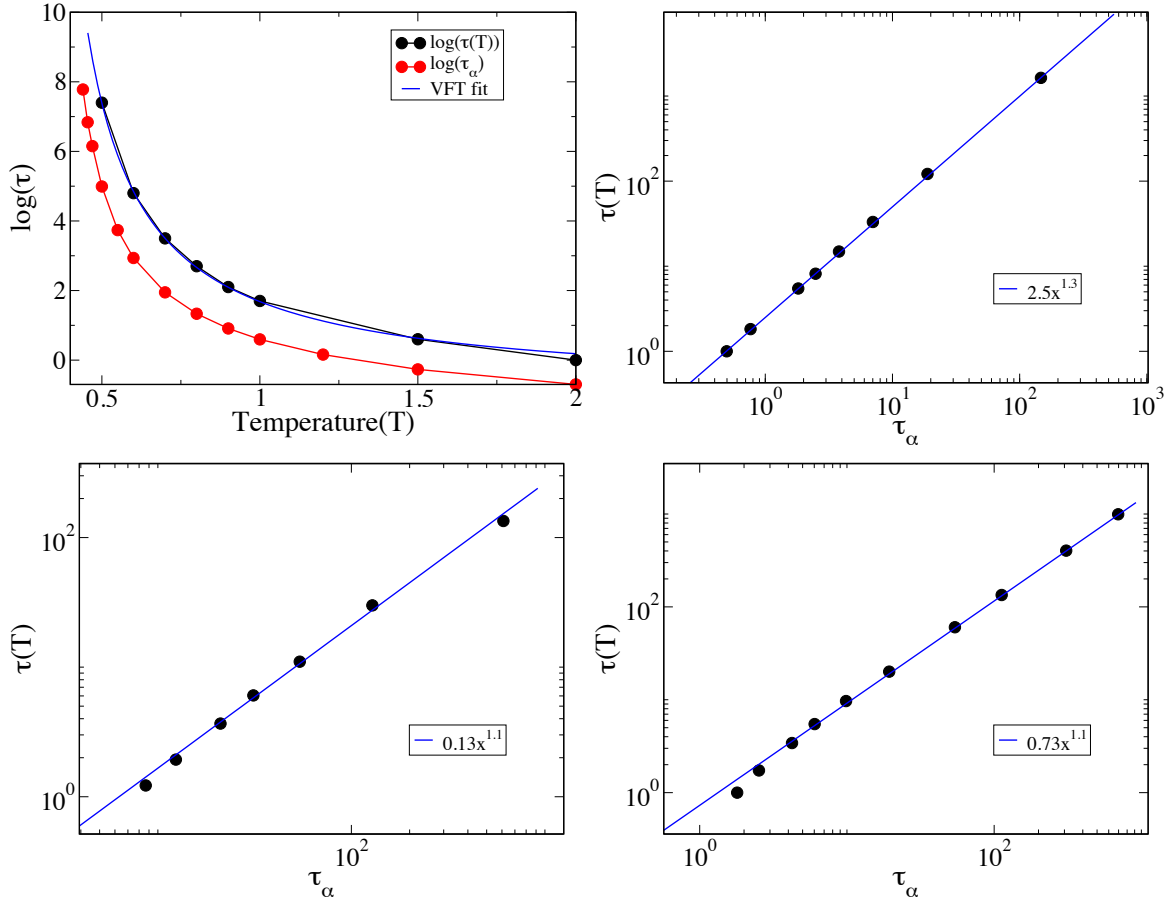


FIG. 10. Top-left panel: Temperature dependence of scaling factor $\tau(T)$ fitted with the Vogel-Fulcher-Tammann (VFT) law along with the temperature dependence of structural relaxation time τ_α . Other panels: Power law relation between $\tau(T)$ and τ_α i.e. $\tau(T) \sim \tau_\alpha^a$, where $a = 1.3$ for 3dKA model (top-right) and $a = 1.1$ for both 3dHP model (bottom-left) and 2dmKA model (bottom-right).

for a fixed length of the probe molecules, we check the temperature dependence of FPT distribution for a fixed rod length. As argued earlier the skewness of distribution $P(\log(t))$ shouldn't change with change in temperature for spatially homogeneous diffusion process, but in supercooled liquid it will show significant changes. For large enough rods this again shouldn't change even at low temperatures, because of averaging effect at larger volume. So one can use the temperature scaling obtained by

collapsing $P(\log(t))$ of larger rods to subtract the obvious temperature scaling from $P(\log(t))$ for smaller rods to see the effect of growing structural order. Although it is clear from the value of χ_{FPT} without any rescaling. Thus increase in skewness (χ_{FPT}) of $P(\log(t))$ for a rod of fixed length immersed in a liquid of decreasing temperature would be direct evidence of growing structural length scale. In Fig:9(left & center) the unscaled and scaled FPT distribution $P(\log(t))$ (scaled with $\tau(T)$) for rod of length $L_{rod} = 4.9$ are shown (3dKA model). The scaling thus obtained $\tau(T)$ is used in Fig: 9(right) for rod of length $L_{rod} = 2.8$ which collapses the large time part of the distributions well and extra small time shoulder is a measure of growing structure at the length scale of rod. The growth of χ_{FPT} with decreasing temperature is shown in the inset of Fig: 9(right).

In Fig:10, we have shown the temperature dependence of $\tau(T)$. The solid line passing through the data points is a fit using the Vogel-Fulcher-Tammann (VFT) law defined as $\tau \sim \tau_{\infty} \exp[A/(T - T_{VFT})]$, which gives good fit to data over a large window of relaxation time τ_{α} in various supercooled liquids. The VFT divergence temperature, T_{VFT} comes out to be $T_{VFT}^{rod} \simeq 0.273$ which is very close $T_{VFT} \simeq 0.296$ of the host supercooled liquid medium. Moreover $\tau(T)$ and τ_{α} are related to each other via power law see Fig: 10 (top-right & bottom panel), although the power with which both are related doesn't seems to be universal. It suggests that the VFT divergence is actually same within error bar. Thus it is clear that rotational correlation time of the immersed rod can be a very good proxy of the relaxation time of the host liquid medium.

VII. ANALYSIS OF EXISTING EXPERIMENTS

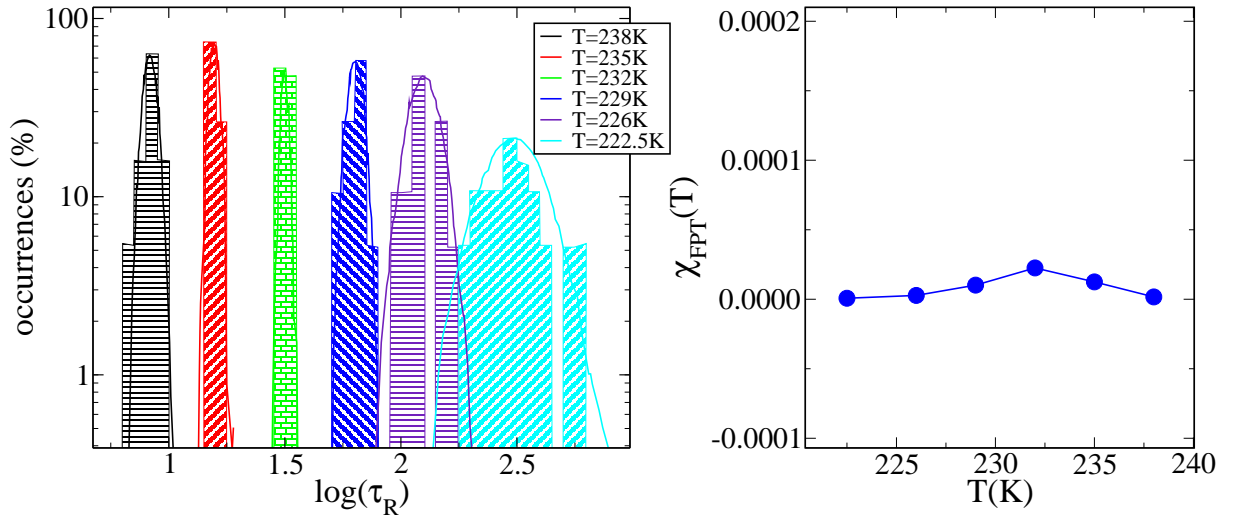


FIG. 11. Left panel: Distribution of correlation time of gold nano rods immersed in supercooled glycerol at different temperatures. Data taken from [7]. Right panel: Temperature variation of negative of skewness $\chi_{FPT}(T)$ of FPT distribution. One can clearly see that skewness hardly changes for gold nano rods.

The existing experimental studies [7, 8] also uses the same distribution $P(y = \log(\tau_R))$ where τ_R is the decorrelation time of the single dye molecule ($\sim 1nm$) [8] and gold nano rod ($\sim 30nm$) [7] immersed in supercooled glycerol at different temperatures. As argued earlier, if the medium is homogeneous (not supercooled), then the distribution should be same at different temperatures except the shift in mean. This is clearly not the case for the experiments with dye molecule, and the appearance of shoulder at small time is clearly visible (see the discussion in main article). For the experiments with nano-rod which is much larger in size than the dye molecules, the changes in skewness is much smaller Fig:11 in complete accordance with the simulation results.

VIII. MODEL SYSTEMS

3dKA Model: 3dKA (3d-Kob-Anderson) model [9] is the famous 80:20 binary mixture of A and B type Lennard-Jones particles. The interaction potential is given by

$$V_{\alpha\beta}(\mathbf{r}) = 4\epsilon_{\alpha\beta} \left[\left(\frac{\sigma_{\alpha\beta}}{r} \right)^{12} - \left(\frac{\sigma_{\alpha\beta}}{r} \right)^6 \right] \quad (32)$$

where α and β varies in A, B and the interaction strengths and radii are $\epsilon_{AA} = 1.0$, $\epsilon_{AB} = 1.5$, $\epsilon_{BB} = 0.5$; $\sigma_{AA} = 1.0$, $\sigma_{BB} = 0.88$ and $\sigma_{AB} = 0.8$. The interaction is truncated at $r = 2.5\sigma_{\alpha\beta}$ and is made smooth by adding upto 4th order terms. The simulations are done in temperature range $T = 0.45, 1.00$ while the pressure is so chosen that the average number density is, $\rho = 1.2$ with 5000 particles.

3dHP Model: 3dHP (3d Harmonic Potential) model [10] is a bridge between the finite- temperature glasses and hard-sphere glasses and is usually studied in context of jamming. It is a 50:50 binary mixture of harmonic spheres with diameter ratio 1.4 and interacting via potential,

$$V_{\alpha\beta}(\mathbf{r}) = \epsilon \left[1 - \left(\frac{r_{\alpha\beta}}{\sigma_{\alpha\beta}} \right) \right]^2 \quad (33)$$

for $r_{\alpha\beta} < \sigma_{\alpha\beta}$ and $V_{\alpha\beta} = 0$ otherwise, where $\sigma_{\alpha\beta} = \frac{(\sigma_{\alpha} + \sigma_{\beta})}{2}$ and $\epsilon = 1$. Again as in 3dKA, its pressure is chosen to keep average number density, $\rho = 0.82$ with $N=5000$, while the temperature is varied between $\{T = 0.0050, 0.0090\}$

2dMKA: 2dMKA (2d Modified Kob-Anderson) model [11] is the glass forming model in 2 dimensions which have properties like 3dKA. It is 65:35 binary mixture of same A and B particles of 3dKA model interacting with exactly the same potential and parameters. Temperature range looked upon for this model is $\{T = 0.47, 1.50\}$ with $N=1000$.

Rods: In all of the glass formers mentioned above we have added few (two in 3dKA and one in 3dHP, 2dMKA) rigid rods made up of variable number of spheres N , each separated by a fixed distance from the other by a distance of $0.3\sigma_{AA}$, where σ_{AA} is the diameter of the largest particle type (A) for 3dKA and 2dmKA models. For 3dHP model we used $0.42\sigma_{AA}$. Each sphere in a rod have same mass and interacts via same potential as parent spheres with $\sigma_{RodSphere} = 1$, $\epsilon_{RodSphere} = 1$, $\sigma_{RodRod} = 1$ and $\epsilon_{RodRod} = \frac{1}{2}$ same for all models. $\epsilon_{RodRod} = \frac{1}{2}$ is chosen to avoid the chance of rods sticking together along there length.

-
- [1] C. Dasgupta, A. V. Indrani, S. Ramaswamy, M. K. Phani, Is there a growing correlation length near the glass transition? *Europhysics Letters (EPL)* **15**, 307–312 (1991).
 - [2] L. Berthier, G. Biroli, J.-P. Bouchaud, L. Cipelletti, W. van Saarloos, eds., *Dynamical Heterogeneities in Glasses, Colloids, and Granular Media* (Oxford University Press, 2011).
 - [3] G. Biroli, J.-P. Bouchaud, A. Cavagna, T. S. Grigera, P. Verrocchio, Thermodynamic signature of growing amorphous order in glass-forming liquids. *Nature Physics* **4**, 771-775 (2008).
 - [4] S. Karmakar, E. Lerner, I. Procaccia, Direct estimate of the static length-scale accompanying the glass transition. *Physica A: Statistical Mechanics and its Applications* **391**, 1001–1008 (2012).
 - [5] R. Jain, K. L. Sebastian, Diffusing diffusivity: Rotational diffusion in two and three dimensions. *The Journal of Chemical Physics* **146**, 214102 (2017).
 - [6] M. Doi, *The Theory of Polymer Dynamics (International Series of Monographs on Physics)* (Oxford University Press, 1988).
 - [7] H. Yuan, S. Khatua, P. Zijlstra, M. Orrit, Individual gold nanorods report on dynamical heterogeneity in supercooled glycerol. *Faraday Discussions* **167**, 515 (2013).
 - [8] R. Zondervan, F. Kulzer, G. C. G. Berkhoult, M. Orrit, Local viscosity of supercooled glycerol near T_g probed by rotational diffusion of ensembles and single dye molecules. *Proceedings of the National Academy of Sciences* **104**, 12628–12633 (2007).
 - [9] W. Kob, H. C. Andersen, Testing mode-coupling theory for a supercooled binary lennard-jones mixture i: The van hove correlation function. *Phys. Rev. E* **51**, 4626–4641 (1995).
 - [10] C. S. O'Hern, S. A. Langer, A. J. Liu, S. R. Nagel, Random packings of frictionless particles. *Phys. Rev. Lett.* **88**, 075507 (2002).
 - [11] R. Brüning, D. A. St-Onge, S. Patterson, W. Kob, Glass transitions in one-, two-, three-, and four-dimensional binary lennard-jones systems. *Journal of Physics: Condensed Matter* **21**, 035117 (2008).